Influence of nucleon–nucleon correlations on the basic properties of nuclei and particle–nucleus and nucleus–nucleus interactions

A. N. Antonov and I. Zh. Petkov
Institute of Nuclear Research and Nuclear Power, Bulgarian Academy of Sciences, Sofia, Bulgaria

Fiz. Elem. Chastits At. Yadra **22**, 801–838 (July–August 1991)

This review presents the results of theoretical investigations into the influence of short-range nucleon–nucleon correlations on the basic properties of nuclei and nuclear reactions in approaches that do not use the mean-field approximation. The question is considered in detail in the framework of the generator-coordinate method, the coherent density-fluctuation model (CDFM), and the natural-orbital method. Special attention is devoted to study of the momentum and density distributions of the nucleons in nuclei on the basis of the functional relationships between them. The momentum distributions of two-nucleon clusters in nuclei are also considered. Also discussed are the spectral functions and widths of deep nuclear hole states, the energies and density distribution of the nucleons in the ground state and excited collective monopole states, the occupation numbers, and the natural orbitals in various correlation approaches. The part played by correlations is analyzed for some particle–nucleus and nucleus–nucleus interactions such as elastic and inelastic scattering of electrons and protons and the elastic scattering of α particles and heavier ions.

INTRODUCTION

To analyze a large proportion of modern nuclear experiments at both at high and low energies, it is necessary to go beyond the limit of applicability of the mean-field approximation. This is the case for deep inelastic scattering of protons by nuclei and inclusive and exclusive electron–nucleus scattering. These processes reveal the presence of high-momentum components of the momentum distributions of the nucleons in nuclei, a partial decrease in the level population below the Fermi level and partial occupation of levels above this level in the nuclear ground state, the presence of large widths of deep hole states, and more. These results do not agree with the predictions of the shell model. It is especially worth studying two basic nuclear characteristics, namely, the momentum and density distribution of the nucleons in the nuclei. In principle, these distributions are determined by one and the same many-particle wave function, represented in different spaces. The exact nuclear wave function (as a solution of the many-particle problem) makes it possible to determine both the momentum and the density distribution in the system, as well as the exact connection between them. However, the presence of short-range nucleon–nucleon correlations, tensor correlations, etc., which result from specific features of the nucleon–nucleon forces, coupled with the fundamental difficulties in solving many-particle problems, makes it necessary to use approximations to find the wave function. In various nuclear models, these approximations make it impossible to give a correct description of the density and momentum distributions simultaneously. A typical example is provided by the approaches developed in the framework of the Hartree–Fock approximation (see, for example, Ref. 1), which do not include a significant proportion of the dynamical short-range nucleon–nucleon correlations. In these approaches, the achievement of a correct description of the density distribution leads to failures in determination of the nucleon momentum distribution,[2–4] which is sensitive to dynamical correlations. It is therfore necessary to develop approaches that go beyond the mean-field approximation by taking into account appropriately the nucleon correlations in the nuclei.

In this review, we consider some basic theoretical correlation approaches. We discuss in detail the generator-coordinate method, the coherent density-fluctuation model (CDFM), and the natural-orbital method in nuclear theory. Section 2 is devoted to the influence of nucleon–nucleon correlations on basic nuclear characteristics such as the nucleon momentum and density distributions, the energies and densities of nuclei in the ground state and in excited collective states, the spectral functions of deep hole states, the occupation numbers, and natural orbitals. The influence of correlations on the cross sections for elastic and inelastic scattering of electrons and protons by nuclei and for elastic scattering of α particles and heavier nuclei are discussed in Sec. 3. The main results are briefly summarized at the end.

1. THEORETICAL APPROACHES THAT GO BEYOND THE MEAN-FIELD APPROXIMATION

Need for the construction of nuclear correlation approaches

Analysis of the particle–nucleus interactions mentioned in the Introduction requires detailed study of the nucleon momentum distribution, which depends strongly on the nature of the nuclear forces.[5] The form of the nucleon momentum distribution $n(k)$ at momenta $k \leqslant k_F$ (where k_F is the Fermi momentum) is determined by the attractive part of the nucleon–nucleon forces at large distances. The behavior of $n(k)$ at momenta $k > k_F$ depends on the repulsive core of the forces at short distances. It is therefore to be expected that the high-momentum compo-

 0090-4759/91/040388-18$04.00

nents of the nucleon momentum distributions in nuclear matter and in finite nuclear systems will be similar.

The nuclear shell model gives reasonable results for $n(k)$ when $k \leqslant k_F$, the nucleon momentum distribution in this case being weakly sensitive to the correlations. However, for $k > k_F$ the presence of correlations leads to a behavior of the momentum distributions that does not agree with the predictions of this model. Qualitatively, the reason for this is that the potential of the shell model is smooth, and the corresponding wave functions do not contain high-momentum components. This model does not allow large momenta to arise from the encounter of two particles. The situation in the Hartree–Fock method is similar. Overall, the calculations in this method reproduce satisfactorily nuclear characteristics such as the binding energies, density distributions, radii, etc. However, the results for the momentum distributions are similar to those of the shell model and differ from the experimental data when $k > k_F$. The main reason for this is that the single-determinant wave function of the system does include correlations associated with the Pauli principle but does not contain all the significant effects of short-range nucleon–nucleon correlations. According to Ref. 6, the realistic behavior of $n(k)$ at large momenta is a consequence of correlations contained in a nuclear wave function Ψ of nondeterminant type.

As was shown in Refs. 3 and 7, an appropriate criterion for proximity of the exact single-particle density matrix

$$\rho(\mathbf{r},\mathbf{r}') = A \int \Psi^*(\mathbf{r},\mathbf{r}_2...)\Psi(\mathbf{r}',\mathbf{r}_2...)d\mathbf{r}_2 d\mathbf{r}_3...d\mathbf{r}_A \qquad (1)$$

to the single-particle density matrix $\rho_0(\mathbf{r},\mathbf{r}')$ corresponding to a single-determinant wave function of the system is the requirement of minimality of the mean-square deviation of these two matrices:

$$\mathrm{Tr}[(\rho - \rho_0)^2] = \min. \qquad (2)$$

It was shown in Ref. 7 that this condition is satisfied when $\rho_0(\mathbf{r},\mathbf{r}')$ corresponds to a single-determinant wave function constructed from natural orbitals, i.e., single-particle functions $\varphi_\alpha(\mathbf{r})$, for which the exact single-particle density matrix has the form[8]

$$\rho(\mathbf{r},\mathbf{r}') = \sum_\alpha n_\alpha \varphi_\alpha^*(\mathbf{r})\varphi_\alpha(\mathbf{r}'). \qquad (3)$$

In (3), n_α are the occupation numbers of state α, and $0 \leqslant n_\alpha \leqslant 1$, $\Sigma_\alpha n_\alpha = A$, where A is the mass number.

Solution of the many-particle problem in the Hartree–Fock approximation leads to a single-particle density matrix $\rho_0^{HF}(\mathbf{r},\mathbf{r}')$ that, in general, differs from the $\rho_0(\mathbf{r},\mathbf{r}')$ that satisfies (2). As was shown in Ref. 3, use of the Hartree–Fock procedure to make the diagonal elements of the ρ and ρ_0^{HF} consistent, $[\rho(\mathbf{r},\mathbf{r}) \simeq \rho_0^{HF}(\mathbf{r},\mathbf{r})]$, i.e., the attempt to make the density distributions consistent, leads to an increase in the deviation between the nondiagonal elements of these two matrices [$\rho(\mathbf{r},\mathbf{r}')$ and $\rho_0^{HF}(\mathbf{r},\mathbf{r}')$ for $\mathbf{r} \neq \mathbf{r}'$]. Since the nondiagonal elements play an important part in the determination of the nucleon momentum distribution,

$$n(\mathbf{k}) = \int d\mathbf{r}d\mathbf{r}' e^{i\mathbf{k}(\mathbf{r}-\mathbf{r}')}\rho(\mathbf{r},\mathbf{r}'), \qquad (4)$$

it is not possible in the Hartree–Fock method to obtain simultaneously a realistic description of the momentum and density distributions. This is confirmed by the example of the ^{4}He nucleus, for which it has been shown[2] that the single-determinant wave function cannot describe the form factor (or charge density) and momentum distribution of the nucleons in this nucleus.

Main correlation approaches

In some of the theoretical approaches that take into account the short-range nucleon–nucleon correlations, the ground-state wave function $\Psi(\{\mathbf{r}_i\})$ $(i = 1,...,A)$ is constructed on the basis of the wave function $\Phi(\{\mathbf{r}_i\})$ of the shell model. Thus, in Ref. 9 the relation

$$\Psi(\{\mathbf{r}_i\}) = \hat{F}\Phi(\{\mathbf{r}_i\}) \qquad (5)$$

is used to introduce the correlation operator $\hat{F}$, which is determined by the two-nucleon forces.

In the Jastrow approach,[10–13] the many-particle wave function is approximated by a variational wave function that contains central, spin, isospin, tensor, and spin–orbit correlations of a nucleon pair:

$$\Psi(\{\mathbf{r}_i\}) = \left(S \prod_{i>j=1}^{A} \mathscr{F}_{ij}\right)\Phi(\{\mathbf{r}_i\}), \qquad (6)$$

where

$$\mathscr{F}_{ij} = \sum_{p=1}^{8} f^p(r_{ij}) O_{ij}^p \qquad (7)$$

and

$$O_{ij}^{p=1,...,8} = 1,\ (\tau_i\cdot\tau_j),\ (\sigma_i\cdot\sigma_j),\ (\sigma_i\cdot\sigma_j),$$

$$(\tau_i\cdot\tau_j),\ S_{ij},\ S_{ij}(\tau_i\cdot\tau_j),\ L\cdot S,\ L\cdot S(\tau_i\cdot\tau_j).$$

The parameters of the correlation functions $f^p(r_{ij})$ are determined by a requirement of minimal energy of the system.

The influence of nucleon–nucleon correlations on the properties of finite nuclei can also be investigated in the theory of bound clusters, or the so-called exp S method (see, for example, Refs. 6 and 14). In it, the total many-particle wave function is written in the form

$$|\Psi\rangle = \exp(\hat{S})|\Phi\rangle, \qquad (8)$$

where Φ is a determinant of single-particle orbitals, and $S = \Sigma_{n=1}^{A}\hat{S}_n$ is a sum of the operators $\hat{S}_n$, which create n-particle–hole excitations. This theory can be applied in practice only for light nuclei (^{4}He and ^{16}O in Ref. 6), the system of nonlinear coupled equations for the amplitudes relating to $\hat{S}_n$ being solved by a truncation procedure.

High-momentum components of the nucleon momentum distribution for ^{16}O analogous to the components in Ref. 6 were obtained in Ref. 15 on the basis of Brueckner theory for finite nuclei.

We should also mention the approach developed in Ref. 16 to go beyond the mean-field approximation. In it,

each state is approximated by a linear combination of several projected determinants of the Hartree–Fock–Bogolyubov method.

As was shown in Ref. 17, allowance for two-particle correlations also presents a serious difficulty in the time-dependent Hartree–Fock method. The diagrams that take into account the two-particle–two-hole excitations are included in the method by means of an effective density-dependent interaction. However, the neglect of the time dependence of the two-particle correlations in the method introduces an error when high-energy reactions are investigated.

It is interesting to consider the influence of short-range correlations in an exactly solvable schematic one-dimensional model of N bosons that interact through δ-function forces.[18–20] There was found to be a power-law asymptotic behavior of the nucleon momentum distribution,

$$n(q) \sim_{q\to\infty} [\tilde{v}(q)]^2 \frac{1}{q^4}, \tag{9}$$

and of the form factor:

$$F(q) \sim \left(\frac{\tilde{v}(q)}{q^2}\right)^{N-1} \quad \text{for} \quad q/N \gg 1, \tag{10}$$

where $\tilde{v}(q)$ is the Fourier transform of the two-particle potential.

A phenomenological model[22,23] has been proposed for the study of dynamical short-range and tensor nucleon–nucleon correlations in finite nuclear systems in the framework of the method in which correlation effects are investigated by means of a unitary two-particle correlation operator[21] applied to the wave function of a particle pair in a two-particle density matrix.

In infinite nuclear matter, the correlation approaches are associated with study of the mass operator $\Sigma(k,E)$ corresponding to the single-particle Green's function:

$$G(k,E) = \frac{1}{E - (k^2/2m) - \Sigma(k,E)}. \tag{11}$$

If the nucleon–nucleon interaction v admits an expansion of Σ in perturbation theory (in powers of v), it is interesting to consider the terms following the Hartree–Fock term in the various approaches[24] and their influence on the occupation numbers of the single-particle states,[25,26] effective masses, level densities, etc.[26] In the case of realistic nucleon–nucleon forces, when this expansion is invalid, one can make partial summations of diagrams, and this leads to the so-called hole-line expansion of the mass operator (or low-density expansion).[24,27–31] The first term of this expansion is the Brueckner–Hartree–Fock approximation (see, for example, Refs. 24 and 32). The expansion makes possible systematic calculations of the expectation values of the n-particle operators in infinite and finite (see, for example, Ref. 15) nuclear systems.

Generator-coordinate method

The generator-coordinate method (GCM)[33,34] was proposed as a variational method for studying the collective motions of nucleons in nuclei. In it, the total many-particle wave function of a system of A nucleons is expressed in the form

$$\Psi(\mathbf{r}_i,...,\mathbf{r}_A) = \int f(x_1,x_2,...)\Phi(\mathbf{r}_1,...,\mathbf{r}_A;x_1,x_2,...)dx_1dx_2... . \tag{12}$$

The generating function $\Phi(\{\mathbf{r}_i\}; x_1,x_2,...)\,(i=1,2,...,A)$ depends on the radius vectors $\{\mathbf{r}_i\}$ of the particles and on the generator coordinates $x_1,x_2...$. It can be chosen in the form of a Slater determinant constructed from single-particle functions of particles in the potential well of the so-called construction potential, which is characterized by the parameters $\{x_i\}$. The generator (or weight) function $f(x_1,x_2,...)$ is determined by the condition of minimal energy of the system, which leads to the Hill–Wheeler–Griffin equation:

$$\int [\mathscr{H}(x,x') - EI(x,x')]f(x')dx' = 0, \quad x \equiv \{x_i\}. \tag{13}$$

The overlap kernel $I(x,x')$ and the energy kernel $\mathscr{H}(x,x')$ have the form

$$I(x,x') = \langle \Phi(\{\mathbf{r}_i\},x) \,|\, \Phi(\{\mathbf{r}_i\},x')\rangle, \tag{14}$$

$$\mathscr{H}(x,x') = \langle \Phi(\{\mathbf{r}_i\},x) \,|\, \hat{H} \,|\, \Phi(\{\mathbf{r}_i\},x')\rangle, \tag{15}$$

where

$$\hat{H} = \sum_i \frac{\mathbf{p}_i^2}{2m} + \sum_{i<j} v_{ij} \tag{16}$$

is the Hamiltonian of the nuclear system.

It was shown in Ref. 34 that in the case of many fermions the δ-function approximation is valid:

$$I(x,x') \to \delta(x,x'), \tag{17}$$

$$\mathscr{H}(x,x') \to -\frac{\hbar^2}{2m_{\text{eff}}}\delta''(x-x') + \delta(x-x')V\left(\frac{x+x'}{2}\right), \tag{18}$$

and it leads to the Schrödinger equation

$$-\frac{\hbar^2}{2m_{\text{eff}}}f''(x) + V(x)f(x) = Ef(x) \tag{19}$$

for the function $f(x)$. In Eq. (19), m_{eff} is an effective mass, which depends in the general case on the generator coordinates. Note that the linear superposition of the Slater determinants Φ in (12) takes the GCM beyond the range of the Hartree–Fock approximation. The extent to which the nucleon correlations are taken into account depends on the nature and number of the considered generator coordinates.

The GCM has been used in a number of studies (see, for example, Refs. 35–38) of nuclear properties. In Refs. 39–42, it was the basis of an approach developed to calculate the single-particle[39,40] and two-particle[41] momentum distributions, occupation numbers and natural orbitals,[42] and the energies and density distributions[39,40] in the nuclei

^{4}He, ^{16}O, and ^{40}Ca. The single- and two-particle momentum distributions were obtained on the basis of the single- and two-particle density matrices, respectively:

$$\rho(\mathbf{r},\mathbf{r}')=\int\int f^*(x)f(x')I(x,x')\rho(x,x',\mathbf{r},\mathbf{r}')dxdx' \quad (20)$$

and

$$\rho(\xi_1,\xi_2;\xi_1',\xi_2')=\frac{1}{2}\int\int dxdx'f^*(x)f(x')I(x,x') \times[\rho(x,x';\xi_1,\xi_1')\rho(x,x';\xi_2\xi_2') -\rho(x,x';\xi_1,\xi_2')\rho(x,x';\xi_2,\xi_1')], \quad (21)$$

where $\xi_i=(\mathbf{r}_i,\sigma_i,\tau_i)$,

$$\rho(x,x';\xi,\xi')=\sum_{k,l=1}^{A}(N^{-1})_{lk}\varphi_k^*(x,\xi)\varphi_l(x',\xi'), \quad (22)$$

$(N^{-1})_{lk}$ is the matrix that is the inverse of the matrix

$$N_{kl}(x,x')=\sum_{\sigma,\tau}\int d\mathbf{r}\varphi_k^*(x,\xi)\varphi_l(x',\xi), \quad (23)$$

$$I(x,x')=\det(N_{kl}); \quad (24)$$

and $\varphi_l(x,\xi)$ are the proton and neutron single-particle functions that occur in the Slater determinant $\Phi(\{\mathbf{r}_i\},x)$ and correspond to a definite construction potential. In this case, the energy kernel has the form[43]

$$\mathscr{H}(x,x')=\langle\Phi(\{\mathbf{r}_i\},x)\,|\,\Phi(\{\mathbf{r}_i\},x')\rangle\times\int H(x,x',\mathbf{r})d\mathbf{r}, \quad (25)$$

where in the case of equal numbers of protons and neutrons ($N=Z$) and effective Skryme forces (with neglect of Coulomb and spin–orbit interactions) $H(x,x',\mathbf{r})$ has the form[44]

$$H(x,x',\mathbf{r})=\frac{\hbar^2}{2m}T+\frac{3}{8}t_0\rho^2+\frac{1}{16}(3t_1+5t_2)(\rho T+\mathbf{j}^2) +\frac{1}{64}(9t_1-5t_2)(\nabla\rho)^2+\frac{1}{16}t_3\rho^{2+\sigma}. \quad (26)$$

In (26), t_0, t_1, t_2, t_3, σ are parameters of the Skyrme forces, and

$$\rho(x,x',\mathbf{r})=4\sum_{\lambda,\mu=1}^{A/4}(N^{-1})_{\mu\lambda}\varphi_\lambda^*(\mathbf{r},x)\varphi_\mu(\mathbf{r},x'); \quad (27)$$

$$T(x,x',\mathbf{r})=4\sum_{\lambda,\mu=1}^{A/4}(N^{-1})_{\mu\lambda}\nabla\varphi_\lambda^*(\mathbf{r},x)\nabla\varphi_\mu(\mathbf{r},x'); \quad (28)$$

$$\mathbf{j}(x,x',\mathbf{r})=2\sum_{\lambda,\mu=1}^{A/4}(N^{-1})_{\mu\lambda}\{\varphi_\lambda^*(\mathbf{r},x')\nabla\varphi_\mu(\eta,x') -[\nabla\varphi_\lambda^*(\mathbf{r},x)]\varphi_\mu(\mathbf{r},x')\}. \quad (29)$$

The function $f(x)$ in (20) and (21) is a solution of Eq. (13).

Coherent density-fluctuation model

In Refs. 4, 45, and 46, the GCM was taken as the basis for the development of a coherent-fluctuation model for the nuclear density (CDFM). By analogy with the relation (17), it was assumed that for a many-fermion system the generating function satisfies the relation

$$\int\Phi^*(\mathbf{r},\mathbf{r}_2,...,\mathbf{r}_A;x')\Phi(\mathbf{r}',\mathbf{r}_2,...,\mathbf{r}_A;x)d\mathbf{r}_2...d\mathbf{r}_A =\rho_x(\mathbf{r},\mathbf{r}')\delta(x-x'), \quad (30)$$

where $\rho_x(\mathbf{r},\mathbf{r}')$ is the single-particle density matrix of the system described by the function Φ:

$$\rho_x(\mathbf{r},\mathbf{r}')=\int\Phi^*(\mathbf{r},\mathbf{r}_2,...,\mathbf{r}_A;x)\Phi(\mathbf{r}',\mathbf{r}_2,...,\mathbf{r}_A;x)d\mathbf{r}_2...d\eta_A. \quad (31)$$

In the case when $\Phi(\{\mathbf{r}_i\};x)$ corresponds to a state of the system with constant density,

$$\rho_x(\mathbf{r})=\rho_0(x)\theta(x-|\mathbf{r}|), \quad (32)$$

where $\rho_x(\mathbf{r})\equiv\rho_x[\mathbf{r},(\mathbf{r}'=\mathbf{r})]$ and $\rho_0(x)=3A/4\pi x^3$, the radius of a sphere containing all A nucleons (so-called fluctuon) was taken as the generator coordinate x. In this case, following the analogy with the theory of nuclear matter, the density matrix (31) can be written in the form

$$\rho_x(\mathbf{r},\mathbf{r}')=3\rho_0(x)\frac{j_1(k_F(x)\,|\mathbf{r}-\mathbf{r}'|)}{k_F(x)\,|\mathbf{r}-\mathbf{r}'|}\theta(x-\tfrac{1}{2}|\mathbf{r}+\mathbf{r}'|), \quad (33)$$

where

$$k_F(x)=\left(\frac{3\pi^2}{2}\rho_0(x)\right)^{1/3}\equiv\frac{\alpha}{x},\quad \alpha=\left(\frac{9\pi A}{8}\right)^{1/3}.$$

The single-particle density matrix is then determined by a coherent superposition of single-particle density matrices of nuclear matter with different densities $\rho_0(x)$:

$$\rho(\mathbf{r},\mathbf{r}')=\int_0^\infty|f(x)|^2\rho_x(\mathbf{r},\mathbf{r}')dx. \quad (34)$$

The density and momentum distributions of the nucleons have, respectively, the form

$$\rho(\mathbf{r})=\int_0^\infty|f(x)|^2\rho_0(x)\theta(x-|\mathbf{r}|)dx; \quad (35)$$

$$n(\mathbf{k})=\int_0^\infty|f(x)|^2\frac{4}{3}\pi x^3\theta(k_F(x)-|\mathbf{k}|)dx. \quad (36)$$

In principle, the weight function $f(x)$ of the model can be determined from Eq. (19), in which the expression for the energy of nuclear matter with density $\rho_0(x)$ is taken as the potential energy $V(x)$ of the collective motion.[47]

The weight function can be determined from (35) by means of the density distribution $\rho(r)$:

$$|f(x)|^2=-\frac{1}{\rho_0(x)}\frac{d\rho(r)}{dr}\bigg|_{r=x}, \quad (37)$$

this relation holding for monotonically decreasing densities $\rho(r)$.

It was shown in Ref. 48 that in the CDFM the particle–nucleus elastic scattering amplitude has the approximate form

$$A_{00}(\mathbf{q})=\int_0^\infty dx|f(x)|^2A_0(x,\mathbf{q}), \tag{38}$$

where $A_0(x,\mathbf{q})$ is the amplitude for scattering of the incident particle by a fluctuon of radius x, and $\mathbf{q}$ is the momentum transfer.

Natural-orbital method in nuclear theory

As was shown in Refs. 4 and 49, the nature of the single-particle description of nuclear properties in the mean-field approximation can be preserved in correlation approaches by using the natural-orbital method (NOM).[8] In it, the single-particle density matrix $\rho(\mathbf{r},\mathbf{r}')$ has the form

$$\rho(\mathbf{r},\mathbf{r}')=\sum_\alpha n_\alpha\psi_\alpha^*(\mathbf{r})\psi_\alpha(\mathbf{r}'), \tag{39}$$

where $\psi_\alpha(\mathbf{r})$ are the natural orbitals, and n_α are the occupation numbers, satisfying the relations

$$0\leqslant n_\alpha\leqslant 1,\quad \sum_\alpha n_\alpha=A. \tag{40}$$

We note that in the Hartree–Fock approximation $n_\alpha=1$ below the Fermi level and $n_\alpha=0$ above it.

The natural-orbital representation has been used to study nucleon–nucleon correlations, basically by two methods.[4] In the first of them (see, for example, Refs. 3 and 50–53), the natural orbitals are constructed by means of wave functions corresponding to the Woods–Saxon potential in order to reproduce the experimentally observed single-particle energies and distribution of the nuclear density (single-particle potential method[50,51]) or the energy spectrum obtained in self-consistent Hartree–Fock calculations.[3,52,53] The occupation numbers are obtained either from analysis of reactions with nucleon transfers[50] or from theoretical calculations that take into account nucleon correlations of different types.[3,52,53] In the second method, one diagonalizes the single-particle density matrix $\rho(\mathbf{r},\mathbf{r}')$ obtained in various correlation approaches [for example, in the Jastrow method for ^{40}Ca (Ref. 56), in the CDFM[49] for ^{16}O, ^{40}Ca, ^{58}Ni, and ^{208}Pb, and in the GCM[42] for ^{4}He, ^{16}O, ^{40}Ca (see Sec. 2)]. It should be emphasized that the natural orbitals and occupation numbers obtained in this manner are determined on a unified basis and are mutually consistent, in contrast to the results of the first method.

2. NUCLEON–NUCLEON CORRELATIONS AND BASIC CHARACTERISTICS OF NUCLEAR SYSTEMS

Nucleon momentum and density distributions

In this section, we discuss the influence of nucleon–nucleon correlations on the nucleon momentum and density distributions, and also the connection between these basic characteristics of the nucleus. As is well known, the local nucleon density distribution $\rho(\mathbf{r})$ is a fundamental characteristic for experimental and theoretical investigations because of its relation to basic nuclear properties such as the shape and size of the nucleus, the binding energy, etc. The nuclear density also plays an important part as a fundamental dynamical variable in the theory. The use of $\rho(\mathbf{r})$ as a fundamental variable leads to a significant simplification of the theory compared with the description in terms of a many-particle wave function. Examples of theoretical approaches in which $\rho(\mathbf{r})$ plays the part of a dynamical variable are the Thomas–Fermi model (see, for example, Ref. 57), the extended Thomas–Fermi method,[58–60] as well as other phenomenological methods (see, for example, Ref. 47). A very important step in the development of the theory of the density functional is the Hohenberg–Kohn theorem,[61,62] which proves the existence of an energy functional $E[\rho]$ of a system of electrons as a universal and unique density functional. This theorem, which is also valid for a system of nucleons, states that the many-particle wave function and, therefore, all properties of the ground state of the system are unique functionals of the density:

$$\Psi\rightarrow\Psi(\mathbf{r}_1,\mathbf{r}_2,..,\mathbf{r}_A;[\rho])\equiv\Psi[\rho]. \tag{41}$$

The single-particle density matrix $\rho(\mathbf{r},\mathbf{r}')$, found in terms of $\Psi[\rho]$, is also a functional of the density. Thus, as was shown in Refs. 4 and 63, the momentum distribution $n(\mathbf{k})$ (4), which depends on $\rho(\mathbf{r},\mathbf{r}';[\rho])$, is also a unique functional of the density. An example of the functional dependence $n(\mathbf{k};[\rho])$ is the expression obtained in the CDFM for the momentum distribution:[4,45,46]

$$n(\mathbf{k};[\rho])=\frac{4\pi}{3}\frac{4}{A}\left[6\int_0^{\alpha/k}\rho(x)x^5dx-\left(\frac{\alpha}{k}\right)^6\rho\left(\frac{\alpha}{k}\right)\right],$$

$$\int n(\mathbf{k})\frac{dk}{(2\pi)^3}=A, \tag{42}$$

which is valid for monotonically decreasing densities ρ. Note that the momentum distribution (42) has power-law asymptotic behavior $n(k)\underset{k\rightarrow\infty}{\rightarrow}k^{-8}$ under the condition $\rho'|_{r=0}=0$, $\rho''|_{r=0}\neq 0$ in agreement with the conclusions from Refs. 18–20. The result $[n(\mathbf{k})\rightarrow n(\mathbf{k};[\rho])]$ obtained in Ref. 63 makes it possible to formulate a theoretical approach in which $\rho(\mathbf{r})$ and $n(\mathbf{k})$ participate as dynamical variables on an equal footing with allowance for the functional relationship between them. The energy functional

$$\tilde{E}[\rho,n]=E[\rho,n]-E_F\int\rho(\mathbf{r})d\mathbf{r}-\int g(\mathbf{k})[n(\mathbf{k})-n(\mathbf{k};[\rho])]\frac{d\mathbf{k}}{(2\pi)^3} \tag{43}$$

was proposed, and a system of equations for $\rho(\mathbf{r})$, $n(\mathbf{k})$, $g(\mathbf{k})$ and for the Lagrangian multiplier E_F was obtained from the variational principle:

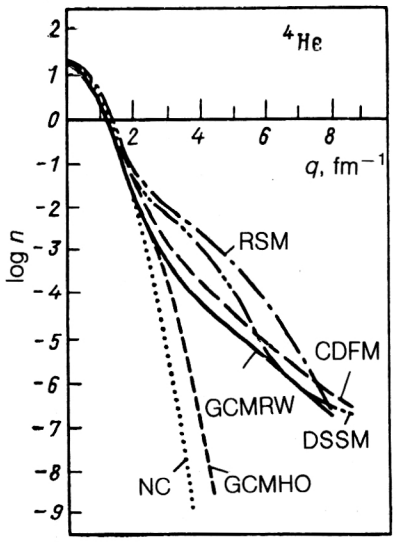

FIG. 1. Momentum distribution of nucleons in ^{4}He according to: CDFM (Ref. 64), GCMRW and GCMHO[39,40] (generator-coordinate method with infinitely deep rectangular well and harmonic-oscillator potential as construction potentials, respectively), RSM and DSSM (exp S method[6] with Reid and de Tourreil–Sprung potentials with soft cores, respectively), and NC (no correlations).[6] The normalization is $\int_0^\infty n(k)k^2dk = A$.

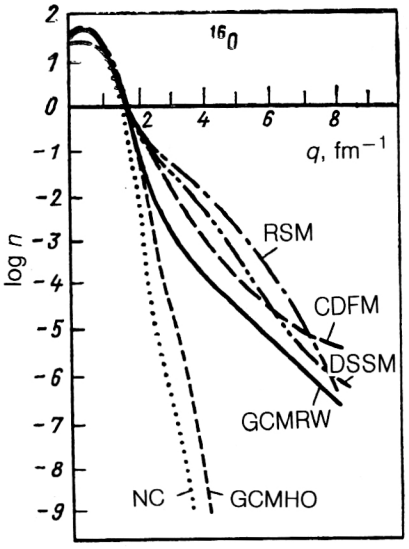

FIG. 2. Momentum distribution of nucleons in ^{16}O (notation as in Fig. 1). The normalization is $\int_0^\infty n(k)k^2dk = A$.

$$\left.\begin{aligned}
&\frac{\delta E}{\delta\rho}=0\rightarrow\frac{\delta E}{\delta\rho}+\int\frac{d\mathbf{k}}{(2\pi)^3}g(k)\frac{\delta n(\mathbf{k};[\rho])}{\delta\rho}=E_{\mathrm{F}},\\
&\frac{\delta E}{\delta n}=0\rightarrow\frac{\delta E}{\delta n}=\frac{g(\mathbf{k})}{(2\pi)^3},\\
&\int\rho(\mathbf{r})d\mathbf{r}=A,\\
&n(\mathbf{k})=n(\mathbf{k};[\rho]).
\end{aligned}\right\}\quad(43a)$$

Use of the functional relationship (42) for $n(\mathbf{k};[\rho])$ in the CDFM and the specific choice of the potential energy $V[\rho]$ from Ref. 47 lead to a satisfactory estimate of the nucleon separation energies in the case of the ^{16}O and ^{40}Ca nuclei.[63]

The results of calculations of the nucleon momentum distribution in the various correlation approaches for the nuclei ^{4}He, ^{12}C, ^{16}O, ^{40}Ca, and ^{208}Pb are shown in Figs. 1–6. The nucleon momentum distributions for ^{4}He and ^{16}O in Figs. 1 and 2 were calculated in the CDFM[64] by means of the relation (42) using a symmetrized Fermi density distribution $\rho(\mathbf{r})$ (Ref. 65) with parameters determined from data on elastic electron–nucleus scattering, in the GCM[39,40] by means of the relations (20), (22)–(24) and the construction potentials of an infinitely deep rectangular well and a harmonic oscillator using Skyrme effective forces, in the exp S method[6] using the Reid nucleon–nucleon potential and the de Tourreil–Sprung potential with soft cores, and in the Hartree–Fock method.[6] The principal characteristic feature of the momentum distributions obtained in the correlation approaches (CDFM, GCM with rectangular construction potential, exp S) is the presence of a high-momentum component at momenta $k\gtrsim 2$ fm^{-1}; this indicates that there is effective allowance for the short-range correlations in these approaches. Figure 3 shows that the results of the CDFM, the exp S method, and the correlation approach of Ref. 66 agree with the experimental data for the nucleon momentum distribution in ^{4}He obtained from ^{4}He(e,e') reactions (see, for example, Ref. 67). It can be seen from Fig. 4 that the results of the correlation approaches (CDFM and the method of Ref. 13) also agree with the data for $n(k)$, including momenta $k\gtrsim 2$ fm^{-1}, in the case of the ^{12}C nucleus.[67,68] Figure 5 compares the theoretical results for $n(k)$ in ^{40}Ca obtained in the shell model with a harmonic-oscillator potential, in a phenomenological model that takes into account tensor and short-range correlations,[23] in the approach of Ref. 13, in the CDFM,[69] and in the natural-orbital method.[51] In the last case, natural orbitals obtained in a single-particle potential[50] and occupation numbers with different percentages of protons above the Fermi level in relation to the total number of protons were used. It was shown that a

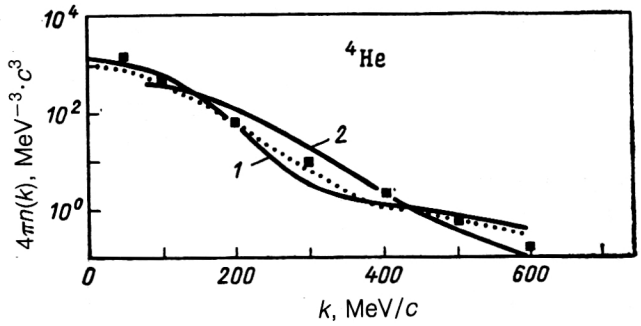

FIG. 3. Momentum distribution of nucleons in ^{4}He. The squares are data from the ^{4}He(e, e') reaction (Ref. 67), the dotted curve is the calculation in the exp S method (Ref. 6), curve 1 is the calculation of Ref. 66, and curve 2 is the calculation in the CDFM.[64] The normalization is $\int n(\mathbf{k})d\mathbf{k} = 1$.

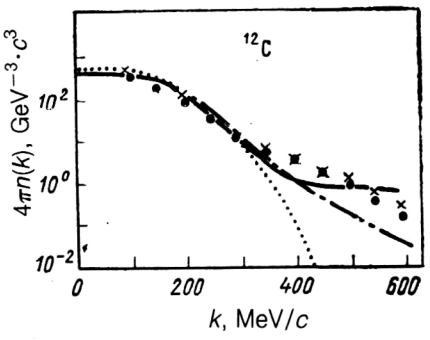

FIG. 4. Momentum distribution of nucleons in ^{12}C. The black circles and crosses are the experimental data taken from Refs. 67 and 68; the continuous curve shows the results of Ref. 13; the chain curve, the results in the CDFM (Ref. 45); the dotted curve gives the results in the Hartree–Fock method. The normalization is $\int n(\mathbf{k})d\mathbf{k} = 1$.

deviation of the occupation numbers from their values in the Hartree–Fock method has a relatively small influence on the behavior of $n(k)$ at large momenta and that the main effect of the short-range correlations is contained in the single–particle functions (natural orbitals). This can be seen in Fig. 5, in which curve 3 gives the result in the NOM, in which the natural orbitals participate in the Slater determinant. Even in this case one can see that there is a significant difference between the high-momentum behavior of $n(k)$ in the NOM and in the shell model (curve 1). The CDFM has also been developed[70] for the case of nonmonotonic charge densities. Figure 6 compares the proton momentum distributions $n_p(k)/Z$ for ^{208}Pb calculated in the CDFM (with charge density from Ref. 71) and in the correlation method of Refs. 3 and 53 with experimental data for $n_p(k)/Z$ in ^{12}C and ^{58}Ni. It can be seen that the results of the CDFM and the approach of Ref. 3 describe the data satisfactorily in the region $1.5 < k < 2.2$ fm^{-1}.

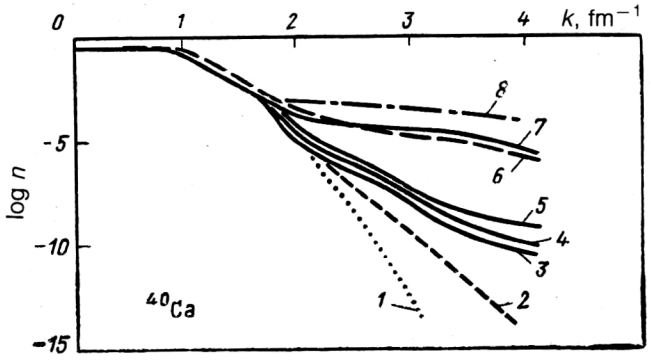

FIG. 5. Momentum distribution of protons in ^{40}Ca: 1) shell model with harmonic-oscillator potential (Ref. 23); 2) and 7) model of Ref. 23 with allowance for tensor correlations (2) and tensor and short-range correlations (7); 3)–5) natural-orbital method[51] based on model of single-particle potentials (Ref. 50); 3) Slater determinant; 4) with 3.55% protons above the Fermi level; 5) with 20.5% protons above the Fermi level; 6) CDFM (Ref. 69); 8) variational approach of Ref. 13. The normalization is $\int n(\mathbf{k})d\mathbf{k} = 1$.

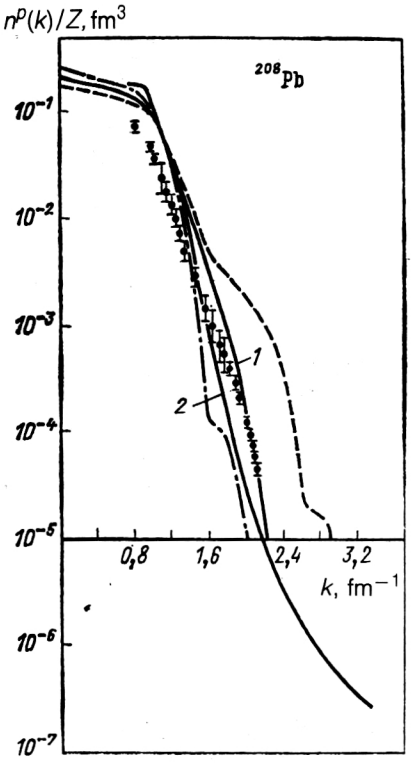

FIG. 6. Momentum distribution $n_p(k)/Z$ of protons in ^{208}Pb: 1) 11.6% protons above the Fermi level; 2) CDFM[70] using the experimental charge distribution from Ref. 71; the chain curve represents the Hartree–Fock distribution (Refs. 3 and 53); the dotted curve corresponds to 20.5% protons above the Fermi level (Refs. 3 and 53); the black circles are the experimental data from Ref. 3. The normalization is $\int n_p(\mathbf{k})d\mathbf{k} = Z$.

It is interesting to consider studies of effects of the finite size of a system on the momentum distributions.[72–75] It was found that even in the case of heavy nuclei these effects are very appreciable.

The influence of a potential of the shell model with attractive and repulsive parts on the behavior of the nucleon momentum distribution at large momenta was investigated in Ref. 76.

The nucleon momentum distributions at finite temperatures were investigated in the CDFM in Ref. 77.

A more complete analysis of the experimental data on the nucleon momentum distributions in nuclei and a comparison with theoretical results are given in Ref. 4.

Two-particle momentum distributions

It was shown in Refs. 78 and 79 that the high-momentum components of the two-particle momentum distributions play an important part in the description of the cross sections of large-angle proton–nucleus scattering. In the case of the ^4He nucleus, the high-momentum components of the two-particle momentum distributions were obtained in the correlation method using soft-core Reid forces.[66]

On the basis of the relations (21)–(29), the two-particle momentum distributions were calculated in the framework of the GCM for the relative motion $[n_{np}^{rel}(q)]$ and the

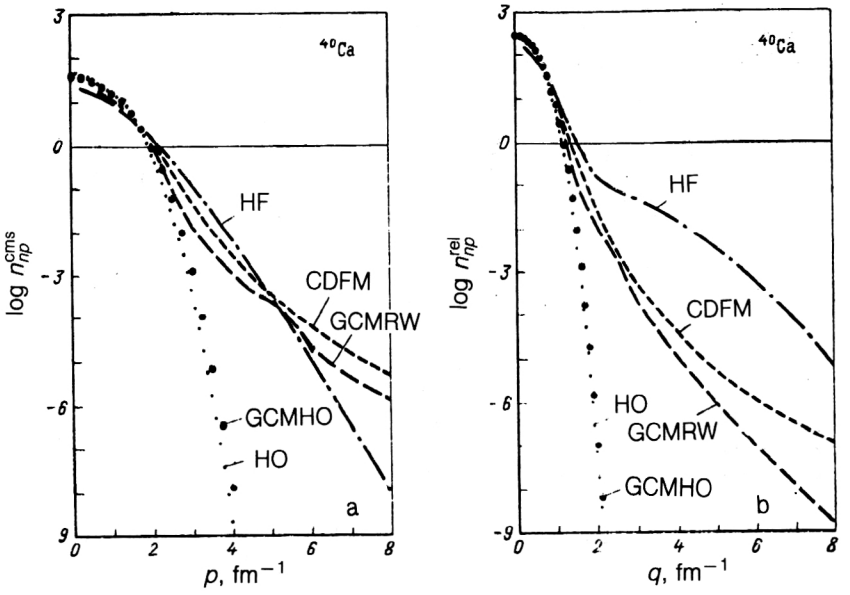

FIG. 7. Two-particle momentum distributions of the center-of-mass motion (a) and relative motion of np pair (b) in ^{40}Ca: harmonic-oscillator model (HO), generator-coordinate method with harmonic-oscillator and rectangular-well potentials as construction potentials (GCMHO and GCMRW, respectively) (Ref. 41); CDFM (Ref. 80); and the result of Ref. 78 (HF). The normalization is $\int n_{np}(\mathbf{k})d\mathbf{k}/(2\pi)^3 = 1$.

center-of-mass motion $[n_{np}^{cms}(p)]$ of a proton–neutron pair in the case of the ^{4}He, ^{16}O, and ^{40}Ca nuclei.[41]

In the CDFM, the following relations for these distributions were obtained[80] in the case of nuclei with $Z=N$:

$$n_{np}^{cms}(p)=A\int_0^\infty dx|f(x)|^2\Omega(x)\left[1-\frac{3|p|}{4k_F(x)}+\frac{|\mathbf{p}|^3}{16k_F^3(x)}\right]\theta\left(k_F(x)-\frac{|\mathbf{p}|}{2}\right); \quad (44)$$

$$n_{np}^{rel}(q)=8A\int_0^\infty dx|f(x)|^2\Omega(x)\left[1-\frac{3|q|}{2k_F(x)}+\frac{|q|^3}{2k_F^3(x)}\right]\theta(k_F(x)-|\mathbf{q}|). \quad (45)$$

Both distributions are normalized to $A^2/4$. In them, $\Omega(x)=4\pi x^3/3$, and $|f(x)|^2$ is determined from (37). Figure 7 gives the two-particle momentum distributions for the ^{40}Ca nucleus calculated in the semiphenomenological model of Ref. 78, in the CDFM,[80] and in the GCM with various construction potentials.[41] It should be noted that, as in the single-particle case, these momentum distributions have a strong dependence on the short-range correlations at momenta greater than 2 fm^{-1}. It was shown in the framework of the GCM with a construction potential in the form of an infinitely deep rectangular well that the distributions $n_{np}^{rel}(q)$ for ^{4}He, ^{16}O, and ^{40}Ca are very close to each other up to $q\lesssim 4$ fm^{-1}. Essentially, we have here the momentum distribution of a deuteron placed in a nuclear medium. Investigating questions related to the nucleon momentum distributions, we should note that, as is well known, the representation of nuclei as consisting of nucleons is valid to momentum transfers of order 1 GeV/c ($\sim$5 fm^{-1}). At momenta above this limit, the subnucleonic degrees of freedom play the main part in particle–nucleus and nucleus–nucleus interactions.

Ground and collective excited states of nuclei in the CDFM and GCM

In the framework of the CDFM, the nuclear dynamics is based on Eq. (19), in which the function $V(x)$ is taken to be the approximate expression for the energy of nuclear matter with density $\rho_0(x)$ in the approach of Brueckner *et al.*[47] The value of the parameter m_{eff} is determined variationally by requiring consistency between the ground-state energies for a large number of nuclei and the experimental energies. It was shown[81,82] that allowance for the dynamics in the CDFM leads to a change in the mean nucleon binding energy from the value 14–16 MeV for nuclear matter to 8–9 MeV for finite nuclei, i.e., to corrections of order $\sim A^{2/3}$ in the von Weizsäcker formula for nuclear binding energies. The properties of "hard" vibrations in the CDFM associated with collective motion of the nucleons were obtained. The energies of the excited 0^+ states ($\hbar\omega_h/2\simeq 19.5^{2/3}$ MeV) are of the order of the nuclear binding energies. A threshold of these excitations was predicted ($A\geqslant 12$ for the first state and $A\gtrsim 70$ for the second). The radii of the nuclei in such excited states are appreciably greater than in the ground state (for ^{40}Ca, $r_{rms}^{(0)}$ = 3.35 fm, $r_{rms}^{(1)}$ = 5.35 fm; for ^{208}Pb, $r_{rms}^{(0)}$ = 5.55 fm, r_{rms} = 7.10 fm, r_{rms} = 10.20 fm), and the density in the central region of the nucleus is reduced. The energies of the 0^+ states in the CDFM agree with calculations for the ^{208}Pb nucleus in the generalized Thomas–Fermi approach.[83] Experimental discovery of the effects of the decay of such states would be interesting. One of the possibilities is associated with isotropic emission of α particles with energy of the order of several mega-electron-volts and neutrons as, for example, occurs when nuclei absorb negative pions.[84] Another possibility is associated with anomalous fission of heavy nuclei with which protons having an energy of several mega-electron-volts interact.[85–90] This process can be interpreted by the possible occurrence of an excited unstable "third fragment" of the type considered in

TABLE I. Energies (MeV) and rms radii (fm) of the ground state and first excited monopole state calculated in the generator-coordinate method.[40]

Nucleus	E_0	$r_{rms}^{(0)}$	E_1	$r_{rms}^{(0)}$	$\Delta E = E_1 - E_0$
^{4}He	−37,06	1,78	−9,83	2,75	27,23
^{16}O	−144,58	2,63	−111,37	2,90	33,21
^{40}Ca	−402,29	3,40	−369,21	3,52	33,71

the CDFM with subsequent fission of the residual nucleus. Such vibrations are possible in any finite system of fermions. For example, in Refs. 91 and 92 the zero-point vibrations of a three-quark nucleon bag in a model analogous to the CDFM were studied. In it, the excitation energy of the Roper resonance, as the first excited breathing state of the bag, is of the order of the excitation energies predicted in the CDFM.

Besides "hard" vibrations, it has been shown to be possible to describe in the CDFM monopole vibrations of breathing type (isoscalar giant monopole resonance) with energies of order $\hbar\omega_M \sim 94A^{-1/3}$ MeV (for $A \gtrsim 40$). They are in qualitative agreement with the results of Ref. 93 ($\hbar\omega \sim 97A^{-1/3}$ MeV) and with the data for certain nuclei, which exhibit a dependence $\sim 80A^{-1/3}$ MeV (Refs. 94–99). Values were obtained for the coefficient of incompressibility K_A for finite nuclei (for ^{16}O, $K_A = 96$ MeV; for ^{40}Ca, $K_A = 216$ MeV; for ^{90}Zr, $K_A = 194$ MeV; for ^{116}Sn, $K_A = 167$ MeV; for ^{140}Ce, $K_A = 196$ MeV; for ^{208}Pb, $K_A = 206$ MeV), and these lead (see Ref. 94) to an estimate of the incompressibility of infinite nuclear matter, $K_\infty \simeq 300$ MeV, in the CDFM. This value agrees with the result $K_\infty = 300 \pm 25$ MeV in Ref. 99.

The energies, rms radii, and densities of the ground and first excited 0^+ states in ^{4}He, ^{16}O, and ^{40}Ca (Table I) were obtained in the framework of the GCM with a construction potential of an infinitely deep rectangular well and with Skyrme forces with parameters $t_0 = -2765.0$, $t_1 = 383.94$, $t_2 = -38.04$, $t_3 = 15865$, and $\sigma = 1/6$ from the relations (13)–(16), (25)–(29).[40]

Spectral functions of deep hole states

Systematic experimental and theoretical investigations of single-nucleon knockout and transfer reactions give information about the validity of the shell model (or a more general quasiparticle approach) for the description of the characteristics of single-particle nuclear states such as the spectral functions, widths and energies of deep hole states, occupation numbers, etc. It is particularly interesting to make a comparative analysis of the values of these quantities for deep hole states and for states close to the Fermi level, doing this for reactions of the type $(e; e'p)$ (see, for example, Refs. 100 and 101) and $(p, 2p)$ (Ref. 102). Information about the spectral function of hole states in the nucleus was obtained. This function is determined by the expression

$$S(E,k) = \langle \Psi_0 | a^+(k)\delta(E - \hat{H})a(k) | \Psi_0 \rangle, \quad (46)$$

where $|\Psi_0\rangle$ is the ground-state wave function of the target nucleus with A nucleons, $a(k)$ is the operator of annihilation of a nucleon with momentum k, E is the energy of the residual nucleus relative to the ground-state energy of the target nucleus, and $\hat{H}$ is the Hamiltonian of the system of $A-1$ nucleons. It was shown[100] that because of the residual interaction the hole state is not an eigenstate of the residual nucleus, but is a mixture of several single-particle states. It is found that the "smearing" of the shell structure leads to broadened maxima of $S(E,k)$, especially for deep states. The expression obtained in Refs. 103 and 104 for $S(E,k)$ is

$$S(E,k) = \sum_{\alpha,\beta} \varphi_\alpha^*(k)\varphi_\beta(k)S(\alpha,\beta,E) \approx \sum_\alpha |\varphi_\alpha(k)|^2 S(\alpha,E), \quad (47)$$

where $S(\alpha,E)$ is the energy distribution of the strength of the hole state α, and $\{\varphi_\alpha\}$ is the complete system of single-particle orbitals generated by the effective potential of the shell model. The experimental data show that the widths of the distribution $S(\alpha,E)$ in the $1s$ hole state reach 40 MeV.

Calculations of the characteristics of deep hole states were made in the quasiparticle–phonon nuclear model (see, for example, Ref. 105) and in other microscopic approaches (see the literature cited in Ref. 105).

The Green's-function method was found to be particularly suitable for studying nuclear spectral functions.[103,106] In a number of studies, this method was used to obtain spectral functions for nuclear matter, after which the results were applied to finite systems by a choice of suitable variables (Refs. 25 and 107–109). This procedure is convenient because the properties of the hole distributions do not depend strongly on the details of the nuclear structure.

In the framework of the CDFM, the following expression was obtained for the spectral function of the hole states:[110]

$$S(k, E \leqslant E_F) = \frac{\pi\alpha}{k[\mu(E - E_F)]^{1/2}} \left| f\left(\frac{\alpha}{k}\left(\frac{E - E_F}{\mu}\right)^{1/2}\right)\right|^2, \quad (48)$$

where $\alpha = (9\pi A/8)^{1/3}$, $|f|^2$ is the weight function in the CDFM (see Sec. 1), μ and E are parameters, and k is

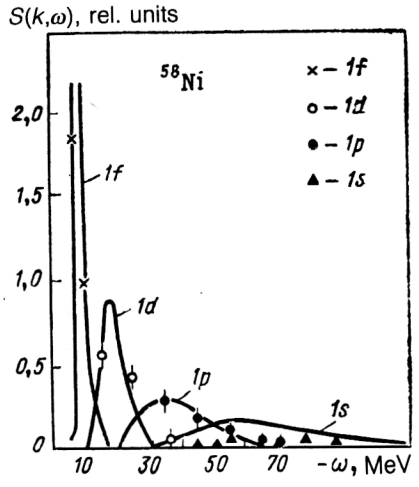

FIG. 8. Comparison of experimental[100] and calculated (in the CDFM[110]) spectral functions in ^{58}Ni (plotted along the ordinate).

interpreted as the momentum in the hole state. The spectral functions obtained in the CDFM for ^{58}Ni (Fig. 8), ^{40}Ca, and ^{28}Si are in good agreement with experimental data from analysis of the $(e,e'p)$ reaction.[100] The widths of the hole states increase on the transition to deeper bound states (for the $1s$ state, they are greater than 40 MeV, in agreement with the experimentally observed widths[100]). The spectral functions, centroid energies, and effective masses considered in Ref. 110 are functionals of the density ρ of the nucleus in the ground state. In the CDFM, the main contributions to the $S(k,E)$ peaks are associated with definite intervals of values of the density. Thus, in the model there is no need to regard the equilibrium density as a free parameter, as is the case in approaches based on the theory of nuclear matter (see, for example, Refs. 107–109).

Natural orbitals and occupation numbers

The natural-orbital method (see Sec. 1) was used to investigate the single-particle aspects of correlation approaches such as the CDFM[49] and GCM.[42] The natural orbitals $\Psi_\alpha(\mathbf{r})$ and occupation numbers n_α were obtained for some nuclei by diagonalizing the single-particle density matrix $\rho(\mathbf{r},\mathbf{r}')$ [of the form (34) in the CDFM and (20) in the GCM]. The following integral equation was solved:

$$\int \rho(\mathbf{r},\mathbf{r}')\Psi_\alpha(\mathbf{r}')d\mathbf{r}'=n_\alpha\Psi_\alpha(\mathbf{r}). \tag{49}$$

For nuclei with total spin $J=0$, the single-particle density matrix should be diagonalized in the $\{ljm\}$ subspace,[50] where l, j, m are the quantum numbers corresponding to the single-particle orbital and total angular momentum and the projection thereof. In the case of spherical nuclei, the natural orbitals are sought in the form

$$\Psi_{nlm}(\mathbf{r})=R_{nl}(r)\,Y_{lm}(\theta,\varphi)=\frac{u_{nl}(r)}{r}Y_{lm}(\theta,\varphi), \tag{50}$$

and this leads to an integral equation for the radial function $u_{nl}(r)$:

$$\int_0^\infty K_l(r,r')u_{nl}(r')dr'=n_{nl}\,u_{nl}(r). \tag{51}$$

The kernel $K_l(r,r')$ is determined by the form of $\rho(\mathbf{r},\mathbf{r}')$ in each particular case. In the GCM, Eq. (51) has nontrivial solutions only for $l\leqslant l_{\max}$, where $l_{\max}$ is the maximal angular momentum of the single-particle states whose wave functions occur in the Slater determinant $\Phi(\{\mathbf{r}_i\};x)$. The natural occupation numbers obtained in the CDFM and GCM (with different construction potentials) are given in Table II. It can be seen that the decrease in the occupation of the levels below the Fermi limit ranges from 0.9% for ^{40}Ca to 1.6% for ^{4}He in the case of the GCM with a rectangular well as the construction potential and is less than 0.5% for the GCM with an oscillator construction potential.

In the case of the CDFM, this value varies between 25.9 and 39.9% for ^{208}Pb, ^{58}Ni, ^{40}Ca, and ^{16}O. A decrease of the level occupations by about 15% was obtained for the ^{40}Ca nucleus in the correlation method of Ref. 25. Analysis of the nucleon momentum distribution in the NOM[51] showed that a decrease of the level occupation below the Fermi limit for ^{40}Ca of order 3–4% was insufficient for a realistic description of the high-momentum components of the nucleon momentum distribution.

As was shown in Sec. 1, diagonalization of the single-particle density matrix makes it possible to obtain consistent natural occupation numbers and single-particle functions in the framework of the CDFM and GCM. As examples, Fig. 9 gives the natural wave functions in the coordinate space for the $2s$ state in the ^{40}Ca nucleus as calculated in both approaches and compared with the functions in the Hartree–Fock approximation found in Ref. 111. The functions differ appreciably in the central region of the nucleus. In the momentum space (Fig. 10), the effects of the nucleon–nucleon correlations are more pronounced in the CDFM and GCM. This result agrees with the behavior of the nucleon momentum distributions. Comparing the occupation numbers and the natural orbitals in the CDFM and GCM, we can assert that in the former the short-range correlations have an effective influence on both the occupation numbers and the wave functions, whereas in the latter the main effect of the correlations is in the wave functions. As was noted in Refs. 4 and 40, allowance for the influence of the correlations on the wave functions is decisive for a correct description of the momentum distributions at large momenta.

To conclude this section, we note that experimental data for the occupation numbers exist for states near the Fermi level for several nuclei of the rare-earth elements[112] and for some lead isotopes.[112,113] As was noted in Ref. 49, these data were obtained by a model-dependent method using single-particle functions from approaches without allowance for nucleon–nucleon correlations. This means that the occupation numbers and wave functions are not determined from a unified consistent scheme that takes into account the correlations.

TABLE II. Natural occupation numbers in the CDFM[49] and in the GCM[42] [with a construction potential in the form of a harmonic-oscillator potential (GCMHO) and rectangular well with infinitely high walls (GCMRW)].

State	^{4}He		^{16}O				^{40}Ca		^{58}Ni		^{208}Pb	
	GCMRW	GCMHO	State	GCMRW	GCMHO	CDFM	GCMHO	CDFM	State	CDFM	State	CDFM
$3s$	0,002	0,001	$2p$	0,013	$<10^{-3}$	0,044	$<10^{-3}$	0,061	$2d$	0,14	$3p$	0,23
$2s$	0,014	0,005	$2s$	0,008	$<10^{-3}$	0,191	$<10^{-3}$	0,073	$1g$	0,22	$1i$	0,30
$1s$*	0,984	0,995	$1p$*	0,986	1,000	0,536	1,000	0,211	$2p$	0,31	$2f$	0,31
			$1s$	0,992	1,000	0,804	1,000	0,442	$1f$*	0,44	$3s$*	0,46
								0,548	$2s$	0,56	$1h$	0,51
								0,768	$1d$	0,66	$2d$	0,53
								0,925	$1p$	0,84	$1g$	0,71
									$1s$	0,96	$2p$	0,75
Decrease of level population below the Fermi limit.	1,6%	0,5%		1,2%	0,1%	39, %	<0,1%	36,6%		35,1%	$1f$	0,85
											$2s$	0,91
											$1d$	0,94
											$1p$	0,99
											$1s$	1,00
				0,9%								25,9%

*Fermi level

The occupation numbers of the single-particle states for nuclei with $A<50$ and their deviations from the values in the Hartree–Fock method were determined in Ref. 114 by an investigation of the densities and charge transition densities of nuclei. However, for the heavy nuclei ^{208,206}Pb and ^{205}Tl it was shown[115] that the charge distributions are not sufficiently informative to reveal the effects of nucleon correlations in these nuclei.

3. NUCLEON-NUCLEON CORRELATIONS AND THE CHARACTERISTICS OF NUCLEAR INTERACTIONS

In this part of the paper, we shall consider some aspects of the investigation of the effects of nucleon–nucleon correlations on the scattering of electrons, protons, and ions by nuclei.

Elastic and quasielastic electron scattering

Electron–nucleus scattering gives important information about the part played by short-range nucleon–nucleon correlations.[116]

Here, we consider the influence of these correlations, which are taken into account in the CDFM in their effect on the charge form factor of the nuclei. It was shown in Ref. 45 that the charge form factor can be represented in the form

$$F(q)=\int_0^\infty dx\,|f(x)|^2F_0(qx), \tag{52}$$

where

$$F_0(qx)=j_1(qx)/qx \tag{53}$$

is the form factor of a fluctuon with radius x, and $j_1(qx)$ is a spherical Bessel function.

In Refs. 117 and 118, a mechanism of electron scattering by fluctons was considered in the high-energy approximation. With allowance for the relation (38), the form factor can be written in the form (52), where

$$F_0(q,x)=\frac{3}{2x^3}\sum_{\varepsilon=\pm1}\frac{G(x,\varepsilon)}{q_{\text{eff}}^2(x,\varepsilon)}\left(x+\frac{i\varepsilon}{q}\right)e^{i[\varepsilon qx+\Phi(x,\varepsilon)]} \tag{54}$$

is the form factor of a fluctuon with radius x in the high-energy approximation.[119,120] The explicit forms of $G(x,\varepsilon)$, $q_{\text{eff}}^2(x,\varepsilon)$, and $\Phi(x,\varepsilon)$ are given in Ref. 116. The cross section for elastic electron–nucleus scattering is determined by the relation

$$\frac{d\sigma}{d\Omega}=\left(\frac{d\sigma}{d\Omega}\right)_{\text{M}}|F(q)|^2, \tag{55}$$

where $F(q)$ is given by Eqs. (52) and (54), $(d\sigma/d\Omega)_{\text{M}}$ is the Mott cross section

$$\left(\frac{d\sigma}{d\Omega}\right)_{\text{M}}=\left(\frac{Ze^2}{2E}\right)^2\frac{\cos^2(\theta/2)}{\sin^4(\theta/2)}, \tag{56}$$

and E is the energy of the incident electrons. The CDFM weight function $|f(x)|^2$ is determined from (37) by means of the density distribution proposed in Ref. 121 and the symmetrized Fermi distribution.[65,116] The results of calculations of the differential cross section for elastic scattering

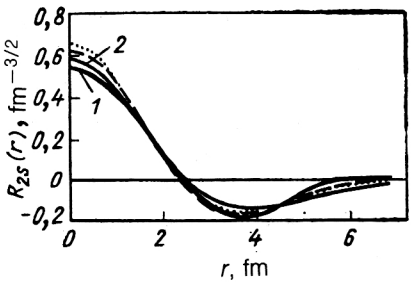

FIG. 9. Natural orbitals in coordinate space for ^{40}Ca ($2s$ state): 1) results of the CDFM[42] with an infinitely deep rectangular well as the construction potential; 2) Hartree–Fock method (Ref. 111); the dotted curve gives the results of the GCM[42] with a harmonic-oscillator construction potential, and the broken curve gives the CDFM results.[49]

of 750-MeV electrons by the ^{40}Ca nucleus and 502-MeV electrons by the ^{208}Pb nucleus are given together with the ^{12}C and ^{16}O form factors in Figs. 11 and 12, where they are compared with experimental data from Refs. 116 and 122. The use of $\rho(\mathbf{r})$ from Ref. 121 and the high-energy approximation in the framework of the CDFM leads to a correct description of the experiments, namely, to better agreement with the data at small angles than for the Born approximation, to partial filling of the diffraction dips, and to a description of the cross sections and form factors up to appreciable momentum transfers (for example, the third maximum of the cross section is described for the nucleus ^{40}Ca, as well as for ^{12}C and ^{16}O, in contrast to the results of Ref. 116 using the high-energy approximation and symmetrized Fermi density). This fact is related to the effects of the short-range correlations taken into account in the CDFM.

Quasielastic electron–nucleus scattering also gives information about the part played by short-range correlations in nuclei. It is found that they have a strong influence on the (e,e') cross section at large energy transfers ω (Ref. 123); this cross section cannot be described in the model of a Fermi gas of noninteracting nucleons.[124] Several theoretical studies (see, for example, Refs. 125–127) have been devoted to the effects of the nucleon–nucleon interaction for description of numerous experiments on the determination of the cross section of quasielastic electron scattering (see, for example, Refs. 123, 128, and 129).

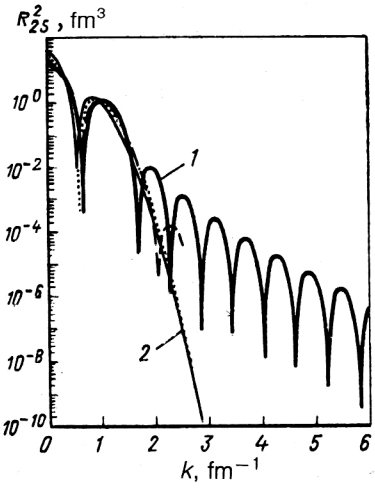

FIG. 10. Natural orbitals in momentum space for ^{40}Ca ($2s$ state). The curves are as in Fig. 9.

In the single-photon approximation, the cross section of the (e,e') process has the form[130]

$$\left(\frac{d^2\sigma}{d\Omega_2 dE_2}\right)_{\text{lab}} = \frac{Z^2}{M_T}\sigma_{\text{M}}[W_2(\mathbf{q}^2,\omega) + 2W_1(\mathbf{q}^2,\omega)\tan^2\theta/2], \quad (57)$$

where M_T and Z are the mass and charge of the target nucleus, σ_{M} is the Mott cross section, $\mathbf{q}$ is the three-dimensional momentum transfer, and $\omega = E_1 - E_2$ (E_1 and E_2 are the energies of the incident and scattered electrons).

In the framework of the CDFM, the nuclear form factors W_1 and W_2 are expressed in the form[131]

$$W_1(\mathbf{q}^2,\omega) = \int_0^\infty dx\,|f(x)|^2 W_1(\mathbf{q}^2,\omega,x); \quad (58)$$

$$W_2(\mathbf{q}^2,\omega) = \int_0^\infty dx\,|f(x)|^2 W_2(\mathbf{q}^2,\omega,x), \quad (59)$$

where $W_i(\mathbf{q}^2,\omega,x)$ $(i=1,2)$ have the same form as the form factors in the independent-particle model,[124] but the Fermi-gas momentum distribution $\theta(k_{\text{F}}-k)$ is replaced by $\theta(k_{\text{F}}(x)-k)$[$k_{\text{F}}(x)$ is the Fermi momentum in Eq. (33) of a flucton of radius x]. Calculations[131] showed that allowance for the correlations in the CDFM leads to a larger cross section at large energy transfers ω than calculations in accordance with the Fermi-gas model and to a general improvement of the agreement with the experimental data at large and small ω (Fig. 13 gives an example for the ^{40}Ca nucleus). Calculations in the CDFM[131] for the longitudinal, $R_L(\mathbf{q}^2,\omega)$, and transverse, $R_T(\mathbf{q}^2,\omega)$, response functions

$$R_L(\mathbf{q}^2,\omega) = \frac{Z^2}{M_T}\frac{\mathbf{q}^2}{q^2}\left[-W_1(\mathbf{q}^2,\omega) + \frac{\mathbf{q}^2}{q^2}W_2(\mathbf{q}^2,\omega)\right], \quad (60)$$

$$R_T(\mathbf{q}^2,\omega) = \frac{Z^2}{M_T}2W_1(\mathbf{q}^2,\omega) \quad (61)$$

(where q is the 4-momentum transfer) using the effective mass $M^* = M_N/1.4$ reveal better agreement with the experimental data for R_L than for the result in the impulse approximation. The theoretical result in the CDFM for the transverse function R_T does not agree with the data in the region of the maximum. The results in the CDFM have a relation to the general problem of response functions. The point is that the longitudinal function is largely determined by the single-nucleon processes, while the transverse function is sensitive to effects of meson exchange currents, particle–hole excitations, meson production, excitation of the Δ resonance, and other factors. The Fermi-gas models describe the transverse functions successfully, while the results for R_L lie above the experimental data. Various

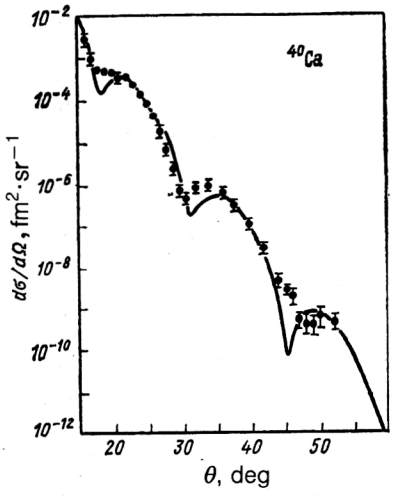

FIG. 11. Differential cross section for elastic scattering of 750-MeV electrons by ^{40}Ca nuclei. The continuous curve is the result of calculation in the high-energy approximation and CDFM[117,118] using the density ρ from Ref. 121; the black circles are the experimental data from Refs. 116 and 122.

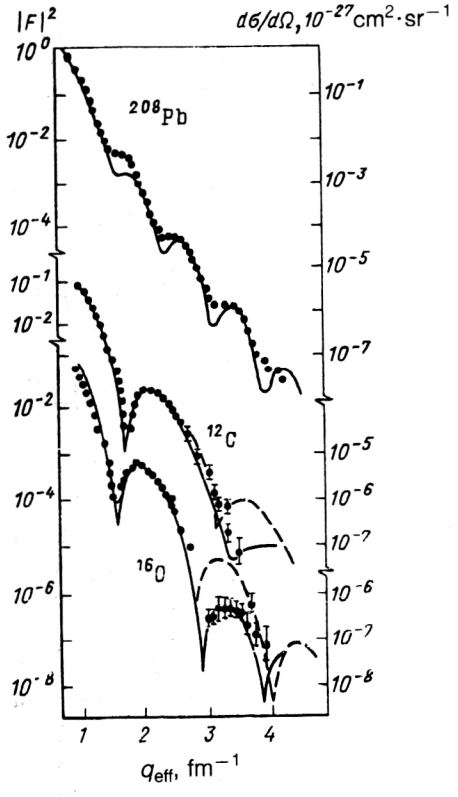

FIG. 12. Form factor of elastic scattering of electrons by ^{12}C and ^{16}O nuclei and differential cross section for elastic scattering of 502-MeV electrons by ^{208}Pb nuclei. The continuous curve shows the result in the high-energy approximation in the framework of the CDFM[117,118] using the density from Ref. 121; the broken curve is the result in the high-energy approximation using the symmetrized Fermi density (Ref. 116); the black circles are the experimental data from Ref. 116.

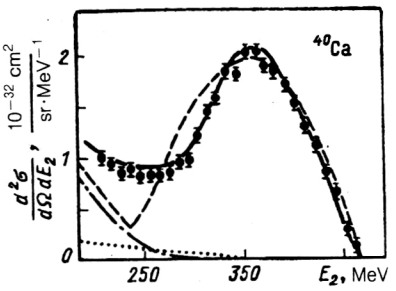

FIG. 13. Differential cross section for quasielastic scattering of 500-MeV electrons by ^{40}Ca nuclei ($\theta = 60°$). The dotted and chain curves are the contributions from pion production (s wave) and from excitation of the Δ isobar, respectively; the broken curve is the total result in the Fermi-gas model (Ref. 129); the continuous curve is the result in the CDFM,[131] with the addition of the contributions of pion production and excitation of the Δ isobar calculated in the Fermi-gas model.[129]

attempts have been made to describe R_L and R_T simultaneously from numerous experiments (see, for example, Refs. 112–138). They are associated with effects like the decrease of the level occupations of the Fermi sea under the influence of the short-range nucleon–nucleon correlations,[139] particle–hole correlations,[140] the increase of the nucleon charge radius in a nuclear medium,[141–145] the influence of meson exchange currents[146] and the Δ resonance,[147] etc. Some nonrelativistic approximations have been used—Hartree–Fock with a density dependence,[148] Tamm–Dancoff,[149] the random-phase approximation,[150,151] the interaction-time approximation,[152] and various relativistic models.[153–155] In most of these studies, the longitudinal function was correctly described, but not the transverse response function. In our opinion, this question is still open in nuclear theory.

Elastic and deep inelastic scattering of intermediate-energy protons

Experimental study of the scattering of intermediate-energy protons by nuclei has particular interest for nuclear-structure theory because of the possibility of obtaining information about dynamical short-range correlations, Pauli correlations, center-of-mass correlations, correlations associated with clustering of nuclear matter, etc.

Although there have been many studies of the effects of correlations on the proton scattering cross sections, this problem remains open. Different, and sometimes contradictory conclusions have been drawn about the influence of correlations on the cross sections, especially on the influence of dynamical short-range nucleon–nucleon correlations. For example, it was concluded in Refs. 156 and 157 that the effects of the correlations are small, and it was shown in Ref. 157 that they amount to 10–12% of the total correlation effect. However, the calculations of other studies (see, for example, Refs. 158–163) indicate that the influence of the correlations on the cross sections cannot be ignored, since it leads to a significant increase in the cross-section peaks [for example, of order 24 and 35% for the

first and second maxima in the case of ^{40}Ca; 9, 23, and 33% for ^{58}Ni; and 15, 23, 30, 37, and 43% for ^{208}Pb (Ref. 159)].

The influence of short-range nucleon–nucleon correlations on the cross section for scattering of 1-GeV protons by ^{40}Ca was studied in Ref. 164 in the framework of the CDFM and Glauber–Sitenko theory (Refs. 165 and 166). The amplitude of the process was expressed in the form (38), where

$$A_0(x,q)=f_p(q)+ik\int J_0(g_qb)\{\exp[i\chi_p(b)]-G_A(x,b)\exp[i\chi_p(x,b)]\}bdb; \qquad (62)$$

$f_p(q)$ and $\chi_p(b)$ are the Coulomb amplitude and Coulomb phase shift for scattering by a point charge Z, $\chi_p(x,b)$ is the flucton Coulomb phase shift, and $G_A(x,b)$ is the nuclear part of the amplitude of one flucton.[167] The calculations were made using realistic charge densities (obtained, for example, from a model-independent analysis[168]). They showed that the cross section in the CDFM differs appreciably from the cross section in the independent-particle model[167] (Fig. 14) and agrees better with the experimental data.

Allowance for the noneikonal corrections to the two-particle proton–nucleon amplitude (in the form of Ref. 169) confirms[170] the conclusions drawn in Ref. 164 about the important role of the CDFM correlations and improves the agreement with the data for large angles ($\theta_{cms}\gtrsim 18°$).

Investigation of high-energy inelastic hadron–nucleus interactions shows that the energy of the inclusive particles reaches values significantly greater than those allowed by the kinematics of a free hadron–nucleon collision. It was suggested that such energy spectra of the particles are due to short-range nucleon–nucleon correlations.[171,172] The experimental data on the production of protons at large angles in proton–nucleus collisions at intermediate energies (600–800 MeV)[173–175] were analyzed under different assumptions about the interaction mechanism.[176,177] In the CDFM, deep inelastic proton scattering has been treated[118,178] in the framework of the single-particle scattering mechanism of Ref. 177, in which the incident proton knocks out a nucleon (with momentum $\mathbf{k}$ in the nucleus) that is observed in the final state with momentum $\mathbf{q}$. The differential cross section of the process[177,179] is calculated by means of the proton momentum distribution $n(\mathbf{k})$ of the target nucleus obtained in the CDFM. In Fig. 15, the calculation in the CDFM is compared with the experimental data and with the results from Ref. 177 for the cross sections of the process $p+{}^{12}\mathrm{C}\to p(180°)+\mathrm{X}$. It can be seen that there is satisfactory agreement with the experimental data, the reason for which is the appreciable difference between the momentum distribution $n(\mathbf{k})$ in the CDFM and $n(\mathbf{k})$ in models with correlations. A similar result was also obtained in Ref. 178 for a relativistically invariant structure function. Use of the nucleon momentum distribution with a high-momentum component for the ^{12}C nucleus from the CDFM and from Ref. 177 leads to a correct description of the angular dependence of the

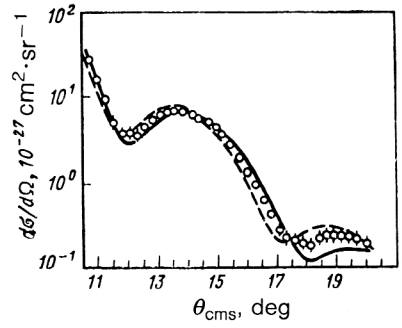

FIG. 14. Differential cross section for elastic scattering of protons (1.04 GeV) by ^{40}Ca. The charge density is from Ref. 168. The continuous curve is the result of the calculation in the CDFM,[164] and the broken curve is the result in the independent-particle model.

polarization of the protons emitted in the process p(640 MeV) $+{}^{12}\mathrm{C}\to p+\mathrm{X}$ (Ref. 180).

It should be noted that the mechanism of proton production at large angles has not yet been fully clarified. The existing models (see, for example, Refs. 78, 79, 176, 177, and 181–184) describe successfully one set or other of the characteristic features of the process. The results of experiments studying coincidences of a proton emitted backward with a proton emitted forward[185,186] present a serious test for the range of applicability of the various mechanisms. It was shown in Ref. 186 that the mechanism of scattering by a two-nucleon cluster in the nucleus can play a more important part than the single-particle mechanism. The energy range in which the single-particle cluster mechanisms of the reaction are valid was established in Ref. 79. However, it is emphasized in Ref. 78 that, irrespective of the differences between the proposed mechanisms, analysis of all known experimental data on inclusive scattering of protons in proton–nucleus collisions confirms that the nucleon momentum distributions contain a high-momentum component associated with nucleon correlations.

Elastic scattering of α particles and heavy ions by nuclei

Experiments on the scattering of α particles of intermediate energies (1.37 GeV) by the ^{12}C nucleus[187] and by the calcium isotopes ^{40,42,44,48}Ca (Ref. 188) make an important contribution to the study of hadron–nucleus and nucleus–nucleus interactions. At the same time, theoretical analysis of the processes in the framework of Kerman–McManus–Thaler theory[189] and in Glauber–Sitenko theory[165,166] made it possible to investigate the influence of short-range correlations on the scattering cross section. It was shown in Ref. 190 that the effects of the correlations in the region of the first diffraction peak are small and increase at large momentum transfers. It was shown in Ref. 191 that the correlations have a small influence on the peaks of the cross section for scattering of α particles by calcium isotopes. However, it was established in Ref. 192 that the effect of the short-range correlations on the second diffraction peak was very large ($\sim$350%). In Ref. 193, the

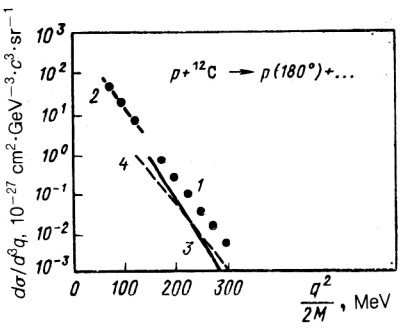

FIG. 15. Differential cross section for inclusive production of protons at angle 180°: 1) result in the CDFM (Refs. 118 and 178); 2) data from Ref. 175 interpolated to 180°; 3) experimental data from Ref. 173; 4) result from Ref. 177.

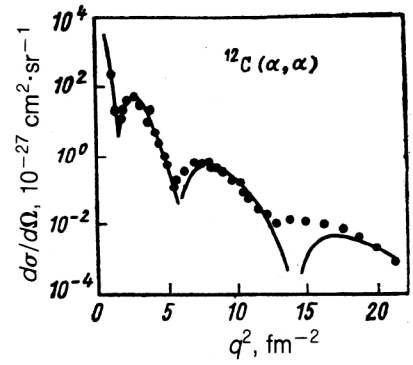

FIG. 16. Differential cross section for elastic scattering of 1.37-GeV α particles by ^{12}C nuclei. The curve gives the result in the CDFM,[48,118] and the black circles are the experimental data from Ref. 187.

corrections to the scattering amplitude associated with nucleon correlations in the case of the nuclei ^{12}C and ^{40}Ca were estimated.

The CDFM was used to analyze α-particle scattering by ^{12}C and calcium isotopes in Refs. 48 and 118. The scattering amplitude was expressed in the form (38), in which the amplitude for scattering by a black body[194] was taken as the amplitude for scattering of a point α particle by a fluctor of radius $x[A_0(x,\mathbf{q})]$. Then the scattering cross section has the form

$$\frac{d\sigma}{d\Omega}=\left(\frac{k_0}{q}\right)^2\left|\int_0^\infty dx|f(x)|^2 xJ_1(qx)\right|^2, \tag{63}$$

where k_0 is the wave number of the incident α particle, q is the momentum transfer, J_1 is a Bessel function, and $f(x)$ is the CDFM weight function, which in the calculations was determined from the relation (37). The CDFM results agree with data on the scattering of α particles by the calcium isotopes and by ^{12}C (Fig. 16), the agreement in the last case being, moreover, appreciably better than in the other approaches (Refs. 187, 190, and 195–197) and comparable with the result of Ref. 193.

To conclude this section, we consider the elastic scattering of heavy ions by nuclei. Analysis of this scattering in the framework of Glauber–Sitenko theory[196,198–201] showed that the influence of the short-range nucleon–nucleon correlations, like that of the correlations associated with the center-of-mass motion, on the cross sections of elastic ion–ion scattering is very appreciable (see, for example, Ref. 201). The effects increase the diffraction peaks (15–20% for the second and 25–35% for the third in the $^{12}C+{}^{12}C$ and $^{16}O+{}^{16}O$ elastic scattering cross sections at energy 2.1 GeV/nucleon).

Elastic scattering of heavy ions was investigated in the CDFM in Refs. 118 and 202. The study used the mechanism of diffraction scattering of a fluctor of the incident nucleus by a black fluctor of the target nucleus with allowance for the contributions of superpositions of fluctors of both nuclei and the Coulomb interaction. The elastic scattering cross section has the form

$$\frac{d\sigma}{d\Omega}=\left|A_{00}(\theta)\right|^2, \tag{64}$$

where

$$A_{00}(\theta)=\int_0^\infty dx_1|f_1(x_1)|^2\int_0^\infty dx_2|f_2(x_2)|^2 A_0(\theta,x_1,x_2), \tag{65}$$

and

$$A_0(\theta,x_1,x_2)=\frac{i}{k}\left\{l_0^{2in+1}\frac{J_1(l_0\theta)}{\theta}+2in\theta^{-2in-2}\int_{l_0\theta}^\infty J_1(z)z^{2in}dz\right\} \tag{66}$$

(see also Refs. 194 and 203). In Eq. (66), k is the length of the wave vector, θ is the scattering angle,

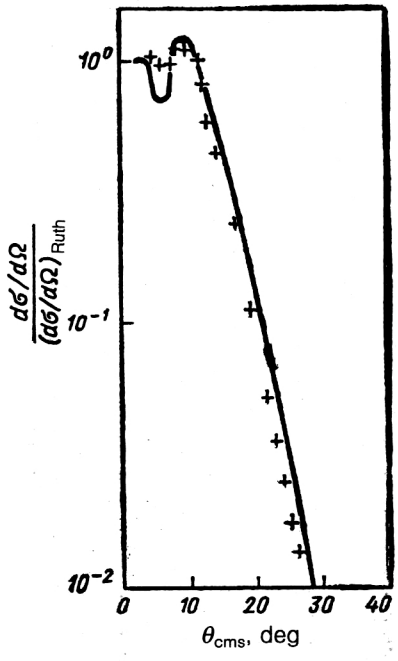

FIG. 17. The ratio $(d\sigma/d\Omega)/(d\sigma/d\Omega)_{Ruth}$ for ^{58}Ni(^{12}C, ^{12}C)^{58}Ni ($E_{lab}=124.5$ MeV) elastic scattering. The continuous curve gives the result in the CDFM,[118,202] and the experimental data are from Ref. 198.

$l_0 = k(x_1 + x_2)$, and $n = Z_1 Z_2 e^2/(\hbar v)$ (v is the velocity of the incident nucleus). The functions $|f_1(x_1)|^2$ and $|f_2(x_2)|^2$ for the incident nucleus and for the target nucleus were determined by means of their density distributions from (37). The proposed approach is valid for small scattering angles ($\theta \ll 1$) and under the condition $l_0 \gg 1$. In Refs. 118 and 202, the ratios of the cross section $d\sigma/d\Omega$ to the Rutherford cross section $(d\sigma/d\Omega)$ were calculated in the CDFM without free parameters for the elastic processes ^{58}Ni(^{12}C, ^{12}C)^{58}Ni ($E_{\text{lab}} = 124$ MeV)$_{\text{Ruth}}$ and ^{209}Bi(^{16}O, ^{16}O)^{209}Bi ($E_{\text{lab}} = 134$ MeV). Satisfactory agreement with the experimental ratios[198,204] was obtained for angles $\theta \ll 1$, at which the diffraction approach is valid [see Fig. 17 for the process ^{58}Ni(^{12}C, ^{12}C)^{58}Ni].

CONCLUSIONS

In this paper, we have considered theoretical approaches that go beyond the mean-field approximation, and we have considered their use in the investigation of nuclear structure and nuclear processes. The approaches include the Jastrow method, the exp S method, the various realizations of the motion of natural orbitals, etc. We have presented in more detail results obtained in the coherent density-fluctuation model, in the generator-coordinate method, and in the natural-orbital method.

On the basis of the Hohenberg–Kohn theorem we have established the existence of a unique functional relationship between the nucleon momentum and density distributions in nuclei. We have proposed a nuclear energy functional of two quantities that are on an equal footing for the theory—the density and momentum distributions of the nucleons. Such a formulation is a generalization of the approaches and models in which only the density or only the momentum distribution is a dynamical variable.

Allowance for intermediate nuclear states with density greater than the equilibrium value in the CDFM and in the GCM (with a construction potential in the form of an infinitely deep rectangular well) makes possible effective inclusion of short-range nucleon–nucleon correlations. In these approaches, high-momentum components of the nucleon momentum distributions are obtained for a large number of nuclei, and they agree with the available experimental data.

In the CDFM, a satisfactory description of the energies of giant isoscalar resonances has been obtained. The possible existence of collective breathing states with high energies has been predicted. Spectral functions of deep hole nuclear states of a number of nuclei in agreement with data from (e,e',p) reactions have been obtained in the framework of the CDFM. A growth in the width of the hole states on the transition to deeper bound states, in agreement with the experimental results, has been established. The experimental results on the EMC effect can be interpreted by means of the spectral functions.[205]

Natural orbitals and occupation numbers of states for various nuclei have been obtained by diagonalizing the single-particle density matrix in the CDFM and GCM.

The influence of the nucleon–nucleon correlations that are taken into account in the CDFM on the cross sections for elastic and quasielastic scattering of electrons, elastic and deep inelastic scattering of protons, as well as elastic scattering of ions is very important for the realistic description of these processes. The results presented here show that a description of the properties of finite nuclear systems at both low and high energies must be sought on a unified basis by methods that go beyond the mean-field approximation.

[1] B. I. Barts, Yu. L. Bolotin, E. V. Inopin, and V. Yu. Gonchar, *The Hartree–Fock Method in Nuclear Theory* [in Russian] (Naukova Dumka, Kiev, 1982).
[2] O. Bohigas and S. Stringari, Phys. Lett. **95B**, 9 (1980).
[3] M. Jaminon, C. Mahaux, and H. Ngô, Phys. Lett. **158B**, 103 (1985); M. Jaminon, C. Mahaux, and H. Ngô, Nucl. Phys. **A473**, 509 (1987).
[4] A. N. Antonov, P. E. Hodgson, and I. Zh. Petkov, *Nucleon Momentum and Density Distribution in Nuclei* (Clarendon Press, Oxford, 1988).
[5] K. Gottfried, Ann. Phys. (N.Y.) **21**, 29 (1963).
[6] J. G. Zabolitzky and W. Ey, Phys. Lett. **76B**, 527 (1978).
[7] D. H. Kobe, J. Chem. Phys. **50**, 5183 (1969).
[8] P.-O. Löwdin, Phys. Rev. **97**, 1474 (1955).
[9] K. A. Brueckner, B. J. Eden, and N. C. Francis, Phys. Rev. **98**, 1445 (1955).
[10] R. Jastrow, Phys. Rev. **98**, 1479 (1955).
[11] S. Fantoni and V. R. Pandharipande, Nucl. Phys. **A427**, 473 (1984); S. Fantoni and S. Rosati, Nuovo Cimento **A20**, 179 (1974).
[12] P. Schiavilla, R. B. Pandharipande, and R. B. Wiringa, Nucl. Phys. **A449**, 219 (1986).
[13] O. Benhar, C. Ciofidegli Atti, S. Liuti, and G. Salmé, Phys. Lett. **117B**, 135 (1986).
[14] H. Kümmel, K. H. Lührmann, and J. G. Zabolitzky, Phys. Rep. **36**, 1 (1978).
[15] J. W. Van Orden, M. Truex, and M. K. Banerjee, Phys. Rev. C **21**, 2628 (1980).
[16] K. W. Schmid, R.-R. Zheng, F. Grümmer, and A. Faessler, Nucl. Phys. **A499**, 63 (1989).
[17] J. W. Negele, Rev. Mod. Phys. **54**, 913 (1982).
[18] R. D. Amado, Phys. Rev. C **14**, 1264 (1976).
[19] R. D. Amado and R. M. Woloshyn, Phys. Lett. **62B**, 253 (1976).
[20] R. D. Amado and R. M. Woloshyn, Phys. Rev. C **15**, 2200 (1977).
[21] J. Da Providencia and C. M. Shakin, Ann. Phys. (N.Y.) **30**, 95 (1964); A. Malecki and P. Picchi, Phys. Lett. **36B**, 61 (1971); Lett. Nuovo Cimento **8**, 16 (1973).
[22] F. Dellagiacoma, G. Orlandini, and M. Traini, Nucl. Phys. **A393**, 95 (1983).
[23] M. Traini and G. Orlandini, Z. Phys. A **231**, 479 (1985).
[24] J. P. Jeukenne, A. Lejeune, and C. Mahaux, Phys. Rep. **25C**, 83 (1976).
[25] H. Orland and R. Schaeffer, Nucl. Phys. **A299**, 442 (1978).
[26] R. Hasse and P. Schuck, Nucl. Phys. **A438**, 157 (1985); **A445**, 205 (1985); S. K. Ghosh, R. Hasse, P. Schuck, and J. Winter, Phys. Rev. Lett. **50**, 1250 (1983).
[27] H. A. Bethe, "Theory of nuclear matter," Ann. Rev. Nucl. Sci. **21**, 93 (1971) [Russ. transl. published as a book, Mir, Moscow, 1974].
[28] K. A. Brueckner, *Theory of Nuclear Matter* [Russ. transl., Mir, Moscow, 1964].
[29] B. D. Day, Rev. Mod. Phys. **39**, 719 (1967).
[30] D. W. L. Sprung, Adv. Nucl. Phys. **5**, 225 (1972).
[31] H. S. Köhler, Phys. Rep. **18C**, 217 (1975).
[32] R. P. Barrett and D. F. Jackson, *Nuclear Sizes and Structure* (Clarendon Press, Oxford, 1977) [Russ. transl., Naukova Dumka, Kiev, 1981].
[33] D. L. Hill and J. A. Wheeler, Phys. Rev. **89**, 1102 (1953).
[34] J. J. Griffin and J. A. Wheeler, Phys. Rev. **108**, 311 (1957).
[35] K. Wildermuth and Y. C. Tang, *A Unified Theory of the Nucleus* (Academic, New York, 1977) [Russ. transl., Mir, Moscow, 1980].
[36] A. M. Lane, *Nuclear Theory: Pairing Force Correlations Motion* (Benjamin, New York, 1964) [Russ. transl., Atomizdat, Moscow, 1967].
[37] W. Bauhoff, Ann. Phys. (N.Y.) **130**, 307 (1980).
[38] Wong Chun Wa, Phys. Rep. **15**, 283 (1975).
[39] A. N. Antonov, Chr. V. Christov, and I. Zh. Petkov, Nuovo Cimento **91A**, 119 (1986).
[40] A. N. Antonov, I. S. Bonev, Chr. V. Christov, and I. Zh. Petkov, Nuovo Cimento **100A**, 779 (1988).

[41] A. N. Antonov, I. S. Bonev, and I. Zh. Petkov, Rapid Communication No. 1[40]-90, JINR, Dubna (1990), p. 35.
[42] A. N. Antonov, I. S. Bonev, Chr. V. Christov *et al., Proc. of the Fourth Workshop on Perspectives in Nuclear Physics at Intermediate Energies, May 8–12, 1989, Trieste, 1989* (World Scientific, Singapore, 1989), p. 300; Nuovo Cimento A (in press).
[43] D. M. Brink, *Proc. of the S.I.F. Course XXXVI*, edited by C. Block (Academic, New York, 1966), p. 247.
[44] H. Flocard and D. Vautherin, Phys. Lett. **55B**, 259 (1975); Nucl. Phys. **A264**, 197 (1976).
[45] A. N. Antonov, V. A. Nikolaev, and I. Zh. Petkov, Bulg. J. Phys. **6**, 151 (1979).
[46] A. N. Antonov, V. A. Nikolaev, and I. Zh. Petkov, Z. Phys. A **297**, 257 (1980).
[47] N. A. Brueckner, J. R. Buchler, R. C. Clark, and R. J. Lombard, Phys. Rev. **181**, 1543 (1969); R. J. Lombard, Ann. Phys. (N.Y.) **77**, 380 (1973).
[48] A. N. Antonov, V. A. Nikolaev, and I. Zh. Petkov, Bulg. J. Phys. **10**, 42 (1983).
[49] A. N. Antonov, Chr. V. Christov, E. N. Nikolov *et al.*, Preprint Nucl. Phys. Lab., OUNP-89-15, Oxford University, Oxford (1989); Nuovo Cimento **102A**, 1701 (1989).
[50] F. Malaguti, A. Uguzzoni, E. Verondini, and P. E. Hodgson, Riv. Nuovo Cimento **5**, 1 (1982).
[51] A. N. Antonov, P. E. Hodgson, and I. Zh. Petkov, Nuovo Cimento **97A**, 117 (1987).
[52] M. Jaminon, C. Mahaux, and H. Ngô, Nucl. Phys. **A440**, 228 (1985).
[53] M. Jaminon, C. Mahaux, and H. Ngô, Nucl. Phys. **A452**, 445 (1986).
[54] J. Dechargè and L. Sips, Nucl. Phys. **A407**, 1 (1983).
[55] V. R. Pandharipande, C. N. Papanicolas, and J. Wambach, Phys. Rev. Lett. **53**, 1133 (1984).
[56] M. Gaudin, J. Gillespie, and G. Ripka, Nucl. Phys. **A176**, 237 (1971).
[57] D. J. Thouless, *The Quantum Mechanics of Many-Body Systems* (Academic, New York, 1972) [Russ. transl., Mir, Moscow, 1975].
[58] O. Bohigas, X. Campi, H. Krivine, and J. Treiner, Phys. Lett. **64B**, 381 (1976).
[59] C. Guet and M. Brack, Z. Phys. A **297**, 247 (1980).
[60] M. Brack, C. Guet, and H.-B. Hakansson, Phys. Rev. **123**, 275 (1985).
[61] P. Hohenberg and W. Kohn, Phys. Rev. **136**, B864 (1964).
[62] W. Kohn and L. J. Sham, Phys. Rev. **140**, A1133 (1965).
[63] A. N. Antonov and I. Zh. Petkov, Nuovo Cimento **91A**, 68 (1986).
[64] A. N. Antonov, I. Zh. Petkov, and P. E. Hodgson, Bulg. J. Phys. **13**, 110 (1986).
[65] V. V. Burov, Yu N. Eldyshev, V. K. Lukyanov, and S. Pol'Yu, Preprint E4-8029, JINR, Dubna (1974).
[66] Y. Akaishi, Nucl. Phys. **A416**, 409 (1984).
[67] C. Ciofi degli Atti, E. Pace, and G. Salmè, Nucl. Phys. **A497**, 361 (1989).
[68] D. B. Day, J. S. McCarthy, Z. E. Meziani *et al.*, Phys. Rev. Lett. **59**, 427 (1987).
[69] A. N. Antonov, V. A. Nikolaev, I. Zh. Petkov, and P. E. Hodgson, Bulg. J. Phys. **10**, 590 (1983).
[70] A. N. Antonov and I. Zh. Petkov, Bulg. J. Phys. **14**, 137 (1987).
[71] B. A. Brown, S. E. Massen, J. I. Escudero *et al.*, J. Phys. G **9**, 423 (1983).
[72] M. Casas, J. Martorell, and Moya de Guerra, Phys. Lett. **167B**, 263 (1986).
[73] J. Hüfner and M. C. Nemes, Phys. Rev. C **23**, 2538 (1981).
[74] M. V. Zverev and E. E. Sapershteĭn, Yad. Fiz. **43**, 304 (1986) [Sov. J. Nucl. Phys. **43**, 195 (1986)].
[75] H. Krivine, Nucl. Phys. **A457**, 125 (1986).
[76] M. Grypeos and K. Ypsilantis, J. Phys. G **15**, 1397 (1989).
[77] A. N. Antonov, J. Kanev, I. Zh. Petkov, and M. V. Stoitsov, Nuovo Cimento **101**, 525 (1989).
[78] Y. Haneishi and T. Fujita, Phys. Rev. C **33**, 260 (1986).
[79] Y. Haneishi and T. Fujita, Phys. Rev. C **35**, 70 (1987).
[80] A. N. Antonov, I. S. Bonev, Chr. V. Christov, and I. Zh. Petkov, Nuovo Cimento **A101**, 639 (1989).
[81] A. N. Antonov, V. A. Nikolaev, and I. Zh. Petkov, *Proc. of the Seventh Intern. Seminar on High-Energy Physics Problems, June 19–23 1984, Dubna*, D1 2-84-599 (Dubna, 1984), p. 606.
[82] A. N. Antonov, V. A. Nikolaev, and I. Zh. Petkov, Nuovo Cimento **86A**, 23 (1985).
[83] N. L. Balazs and H. C. Pauli, Z. Phys. A **281**, 395 (1977).
[84] F. W. Schlepütz, J. C. Comiso, T. C. Meyer, and K. O. H. Ziock, Phys. Rev. C **19**, 135 (1979).
[85] A. I. Yavin, Nucl. Phys. **A374**, 297 (1982).
[86] B. L. Gorshkov, A. I. Il'in, B. Yu. Sokolovskiĭ *et al.*, Pis'ma Zh. Eksp. Teor. Fiz. **37**, 60 (1983) [JETP Lett. **37**, 72 (1983)].
[87] Yu. A. Chestnov, B. L. Gorshkov, A. I. Iljin *et al.*, Preprint No. 941, LNPI, Leningrad (1984).
[88] B. D. Wilkins, S. B. Kaufman, E. P. Steinberg *et al.*, Phys. Rev. Lett. **43**, 1080 (1979).
[89] S. Pandian and N. T. Porile, Phys. Rev. C **23**, 427 (1981).
[90] H. Sauvageon, S. Regnier, and G. N. Siminoff, Phys. Rev. C **25**, 466 (1982).
[91] G. E. Brown, J. W. Durso, and M. B. Johnson, Nucl. Phys. **A397**, 447 (1983).
[92] U.-G. Meissner and J. W. Durso, Nucl. Phys. **A430**, 670 (1984).
[93] K. A. Brueckner, M. J. Giannoni, and R. J. Lombard, Phys. Lett. **31B**, 97 (1970).
[94] N. A. Voinova-Eliseeva and I. A. Mitropol'skiĭ, Preprint No. 1095 [in Russian], Leningrad Institute of Nuclear Physics, Leningrad (1985).
[95] N. A. Voinova-Eliseeva and I. A. Mitropol'skiĭ, Preprint No. 1104 [in Russian], Leningrad Institute of Nuclear Physics, Leningrad (1985).
[96] M. M. Sharma, W. Stocker, P. Gleissl, and M. Brack, Nucl. Phys. **A504**, 337 (1989).
[97] S. Brandenburg, W. T. A. Borghols, A. G. Drentje *et al.*, Nucl. Phys. **A466**, 29 (1987).
[98] W. T. A. Borghols, S. Brandenburg, J. H. Meier *et al.*, Nucl. Phys. **A504**, 231 (1989).
[99] M. M. Sharma, W. T. A. Borghols, S. Brandenburg *et al.*, Phys. Rev. **38**, 2562 (1988).
[100] J. Mougey, M. Bernheim, A. Bussiere De Nercy *et al.*, Nucl. Phys. **A262**, 461 (1976).
[101] N. Nakamura, S. Hiramatsu, T. Kamae *et al.*, Nucl. Phys. **A271**, 221 (1976).
[102] A. N. James, P. T. Andrews, P. Butler *et al.*, Nucl. Phys. **A133**, 89 (1969); A. N. James, P. T. Andrews, P. Kirkby, and B. G. Lowe, Nucl. Phys. **A138**, 145 (1969).
[103] S. Frullani and J. Mougey, Adv. Nucl. Phys. **14**, 1 (1984).
[104] P. E. Hodgson, Rep. Prog. Phys. **38**, 847 (1975).
[105] V. G. Solov'ev, *Nuclear Theory. Quasiparticles and Phonons* [in Russian] (Énergoatomizdat, Moscow, 1989).
[106] D. H. E. Gross and R. Lipperheide, Nucl. Phys. **A150**, 449 (1970).
[107] H. S. Köhler, Nucl. Phys. **88**, 529 (1966).
[108] R. Sartor, Nucl. Phys. **A267**, 29 (1976); **A289**, 329 (1977).
[109] R. Sartor and C. Mahaux, Phys. Rev. C **21**, 2613 (1980).
[110] A. N. Antonov, V. A. Nikolaev, and I. Zh. Petkov, Z. Phys. A **304**, 239 (1982).
[111] R. Muthukrishnan and M. Baranger, Phys. Lett. **18**, 160 (1965).
[112] E. N. M. Quint, B. M. Barnett, A. M. van der Berg *et al.*, Phys. Rev. Lett. **58**, 1088 (1987); M. C. Radhakrishna, N. G. Puttaswamy, H. Nann *et al.*, Phys. Rev. C **37**, 66 (1988).
[113] P. K. A. De Witt Huberts, *Proc. of the Third Workshop on Perspectives in Nuclear Physics at Intermediate Energies, Trieste, May 18–22, 1987* (World Scientific, Singapore, 1988), p. 381.
[114] I. S. Gul'karov and V. I. Kuprikov, Yad. Fiz. **49**, 33 (1989) [Sov. J. Nucl. Phys. **49**, 21 (1989)]; I. S. Gul'karov and M. M. Mansurov, Yad. Fiz. **48**, 1283 (1988) [Sov. J. Nucl. Phys. **48**, 815 (1988)].
[115] L. Bennour, P.-H. Heenen, and P. Bonche, Phys. Rev. C **40**, 2834 (1989).
[116] V. K. Luk'yanov and Yu. S. Pol', Fiz. Elem. Chastits At. Yadra **5**, 955 (1975) [Sov. J. Part. Nucl. **5**, 385 (1975)].
[117] A. N. Antonov, V. A. Nikolaev, and I. Zh. Petkov, C. R. Acad. Bulg. Sci. **34**, 19 (1981).
[118] A. N. Antonov, V. A. Nikolaev, and I. Zh. Petkov, Izv. Akad. Nauk SSSR, Ser. Fiz. **47**, 134 (1983).
[119] D. R. Yennie, F. L. Boos, and D. C. Ravenhall, Phys. Rev. **137**, B882 (1965).
[120] I. Zh. Petkov, V. K. Luk'yanov, and Yu. S. Pol', Yad. Fiz. **4**, 57 (1966) [Sov. J. Nucl. Phys. **4**, 41 (1967)].
[121] V. P. Garistov and I. Zh. Petkov, Bulg. Fiz. Zh. **3**, 6 (1976); A. N. Antonov, V. P. Garistov, and I. Zh. Petkov, Phys. Lett. **68B**, 305 (1977).
[122] J. B. Bellicard, P. Bounin, R. F. Frosch *et al.*, Phys. Rev. Lett. **19**, 527 (1967).
[123] W. Cryż and K. Gottfried, Ann. Phys. (N.Y.) **21**, 47 (1963); S. V.

Dementiĭ, N. G. Afanas'ev, I. M. Arkatov *et al.*, Yad. Fiz. **11**, 19 (1970) [Sov. J. Nucl. Phys. **11**, 10 (1970)]; F. H. Heimlich, M. Köberling, J. Moritz *et al.*, Nucl. Phys. **A231**, 509 (1974).
[124] E. J. Moniz, Phys. Rev. **184**, 1154 (1969).
[125] W. Fabian and H. Arenhovel, Nucl. Phys. **A314**, 253 (1979); A. E. L. Dieperink, T. De Forest, I. Sick, and R. A. Brandenburg, Phys. Lett. **63B**, 261 (1976).
[126] F. A. Brieva and A. Dellafiore, Nucl. Phys. **A292**, 445 (1977); T. De Forest, Nucl. Phys. **A132**, 305 (1969); T. W. Donnely, Nucl. Phys. **A150**, 393 (1970); S. Klawansky, H. W. Kendall, and A. K. Kerman, Phys. Rev. C **7**, 795 (1973); Y. Kawazoe, G. Takeda, and H. Matsuzaki, Prog. Theor. Phys. **54**, 1394 (1975).
[127] R. Rosenfelder, Ann. Phys. (N.Y.) **128**, 188 (1980).
[128] E. J. Moniz, I. Sick, R. R. Whitney *et al.*, Phys. Rev. Lett. **26**, 445 (1971).
[129] R. R. Whitney, I. Sick, J. B. Ficenec *et al.*, Phys. Rev. C **9**, 2230 (1974).
[130] S. D. Drell and J. D. Walecka, Ann. Phys. (N.Y.) **28**, 18 (1964); T. De Forest and J. D. Walecka, Adv. Phys. **15**, 1 (1966).
[131] A. N. Antonov and I. Zh. Petkov, Communication E4-83-663, JINR, Dubna (1983); A. N. Antonov and I. Zh. Petkov, Bulg. J. Phys. **11**, 163 (1984).
[132] C. Marchand, P. Barreau, M. Bernheim *et al.*, Phys. Lett. **153B**, 29 (1985).
[133] P. Barreau, M. Bernheim, M. Brussel *et al.*, Nucl. Phys. **A358**, 287 (1981).
[134] A. Yu. Buki, N. G. Shevchenko, N. G. Afanas'ev *et al.*, Ukr. Fiz. Zh. **28**, 1654 (1983).
[135] M. Deady, C. F. Williamson, J. Wong *et al.*, Phys. Rev. C **28**, 631 (1983).
[136] M. Deady, C. F. Williamson, P. D. Zimmerman *et al.*, Phys. Rev. C **33**, 1897 (1986).
[137] Z. E. Mezziani, P. Barreau, M. Bernheim *et al.*, Phys. Rev. Lett. **52**, 2130 (1984); Phys. Rev. Lett. **54**, 1233 (1985).
[138] R. Altemus, A. Cafolla, D. Day *et al.*, Phys. Rev. Lett. **44**, 965 (1980).
[139] L. S. Celenza, W. S. Pong, M. M. Rahman, and C. M. Shakin, Phys. Rev. C **26**, 320 (1982).
[140] S. Drożdż, G. Co', J. Wambach, and J. Speth, Phys. Lett. **185B**, 287 (1987).
[141] J. V. Noble, Phys. Rev. Lett. **46**, 412 (1981).
[142] P. D. Zimmerman, Phys. Rev. C **26**, 265 (1982).
[143] L. S. Celenza, A. Rosental, and C. M. Shakin, Phys. Rev. C **31**, 232 (1985).
[144] L. S. Celenza, A. Harindranath, and C. M. Shakin, Phys. Rev. C **32**, 248, 650 (1985).
[145] W. M. Alberico, P. Czerski, M. Ericson, and A. Molinari, Nucl. Phys. **A462**, 269 (1987).
[146] M. Kohno and N. Ohtsuka, Phys. Lett. **98B**, 335 (1981).
[147] L. S. Celenza, W. S. Pong, and C. M. Shakin, Phys. Rev. C **27**, 2792 (1983).
[148] M. Kohno, Nucl. Phys. **A410**, 349 (1983).
[149] A. Dellafiore, F. Lenz, and F. A. Brieva, Phys. Rev. C **31**, 1088 (1985).
[150] M. Cavinato, D. Drechsel, E. Fein *et al.*, Nucl. Phys. **A423**, 376 (1984).
[151] U. Stroth, R. Hasse, and P. Schuck, Phys. Lett. **171B**, 339 (1986); Nucl. Phys. **A462**, 45 (1987).
[152] A. Yu. Korchin, É. L. Kuplennikov, and A. V. Shebeko, Yad. Fiz. **44**, 932 (1986) [Sov. J. Nucl. Phys. **44**, 601 (1986)].
[153] K. Wehrberger and F. Beck, Phys. Rev. C **35**, 298 (1987).
[154] G. Do Dang and P. Van Thieu, Phys. Rev. C **28**, 1845 (1983).
[155] G. Do Dang and N. Van Giai, Phys. Rev. C **30**, 731 (1984).
[156] R. D. Viollier and J. D. Walecka, Acta Phys. Pol. **B8**, 25 (1977).
[157] L. Ray, Phys. Rev. C **19**, 1855 (1979).
[158] E. J. Moniz and G. D. Nixon, Ann. Phys. (N.Y.) **67**, 58 (1971).
[159] V. E. Starodubsky, Yad. Fiz. **16**, 946 (1972) [Sov. J. Nucl. Phys. **16**, 522 (1973)]; Nucl. Phys. **A219**, 525 (1974).
[160] E. Boridy and H. Feshbach, Ann. Phys. (N.Y.) **109**, 468 (1977).
[161] A. Chaumeaux, V. Layly, and R. Schaeffer, Ann. Phys. (N.Y.) **116**, 247 (1978).
[162] Z. A. Khan, Z. Phys. A **303**, 161 (1981).
[163] R. Guardiola and E. Oset, Nucl. Phys. **A234**, 458 (1974).
[164] A. N. Antonov, Chr. V. Christov, and I. Zh. Petkov, Z. Phys. A **320**, 683 (1985).
[165] R. J. Glauber, Review paper presented at the Third Intern. Conf. on High Energy Physics and Nuclear Structure, 1969 [Russ. transl., Usp. Fiz. Nauk **103**, 641 (1971)].
[166] A. G. Sitenko, *Theory of Nuclear Reactions* [in Russian] (Énergoatomizdat, Moscow, 1983).
[167] G. D. Alkhazov, Z. Phys. A **305**, 167 (1982).
[168] I. Sick, Phys. Lett. **53B**, 15 (1974).
[169] N. F. Golovanova and V. Iskra, Phys. Lett. **187B**, 7 (1987).
[170] A. N. Antonov, Chr. V. Christov, E. N. Nikolov *et al.*, Preprint ITP-89-46E, Kiev (1989); Z. Phys. A **336**, 333 (1990).
[171] D. I. Blokhintsev, Zh. Eksp. Teor. Fiz. **33**, 1295 (1957) [Sov. Phys. JETP **6**, 995 (1958)]; D. I. Blokhintsev and K. A. Toktarov, Preprint R4-4018 [in Russian], JINR, Dubna (1968).
[172] V. V. Burov, V. K. Lukyanov, and A. I. Titov, Phys. Lett. **67B**, 46 (1977).
[173] S. Frankel, W. Frati, O. Van Dyck *et al.*, Phys. Rev. Lett. **36**, 642 (1976).
[174] S. Frankel, W. Frati, G. Blanpied *et al.*, Phys. Rev. C **18**, 1375 (1978).
[175] V. I. Komarov, G. E. Kosarev, H. Müller *et al.*, Phys. Lett. **68B**, 37 (1977); Communication E1-11513, JINR, Dubna (1978).
[176] H. J. Weber and L. D. Miller, Phys. Rev. C **16**, 726 (1977).
[177] R. D. Amado and R. M. Woloshyn, Phys. Rev. Lett. **36**, 1435 (1976).
[178] A. N. Antonov, V. A. Nikolaev, and I. Zh. Petkov, Communication R4-12207 [in Russian], JINR, Dubna (1979).
[179] G. Jacob and Th. A. J. Maris, Rev. Mod. Phys. **38**, 121 (1966).
[180] R. Ya. Zul'karineev, R. Kh. Kutuev, and Kh. Murtazaev, Yad. Fiz. **32**, 889 (1980) [Sov. J. Nucl. Phys. **32**, 457 (1980)].
[181] T. Fujita, Phys. Rev. Lett. **39**, 174 (1977).
[182] J. Knoll, Phys. Rev. C **20**, 773 (1979).
[183] V. I. Komarov, G. E. Kosarev, H. Müller *et al.*, Nucl. Phys. **A326**, 297 (1979).
[184] Ko Che-Ming and Ta-Chung Meng, Phys. Rev. Lett. **43**, 994 (1979).
[185] V. I. Komarov, G. E. Kosarev, H. Müller *et al.*, Phys. Lett. **80B**, 30 (1978).
[186] Y. Miake, H. Hamagaki, S. Kadota *et al.*, Phys. Rev. C **31**, 2168 (1985).
[187] A. Chameaux, G. Bruge, T. Bauer *et al.*, Nucl. Phys. **A267**, 413 (1976).
[188] A. D. Alkhazov, T. Bauer, R. Bertini *et al.*, Nucl. Phys. **A280**, 365 (1977).
[189] A. K. Kerman, H. McManus, and R. M. Thaler, Ann. Phys. (N.Y.) **8**, 551 (1959).
[190] I. Ahmad, J. Phys. G **6**, 947 (1980).
[191] G. D. Alkhazov, Izv. Akad. Nauk SSSR, Ser. Fiz. **43**, 2115 (1979); Preprint No. 465 [in Russian], Leningrad Institute of Nuclear Physics, Leningrad (1979).
[192] A. Matecki and L. Satta, Preprint LNF-76/36(F), Frascati (1976).
[193] A. S. Pak, A. V. Tarasov, V. V. Uzhinskiĭ, and Ch. Tsérén, Pis'ma Zh. Eksp. Teor. Fiz. **28**, 314 (1978) [JETP Lett. **28**, 288 (1978)]; Yad. Fiz. **30**, 102 (1979) [Sov. J. Nucl. Phys. **30**, 52 (1979)].
[194] A. N. Akhiezer and I. Ya. Pomeranchuk, Usp. Fiz. Nauk **65**, 593 (1958).
[195] R. D. Viollier and E. Turtschi, Ann. Phys. (N.Y.) **124**, 290 (1980).
[196] V. Franko and G. K. Varma, Phys. Rev. C **18**, 349 (1978).
[197] G. Fäldt and I. Hulthage, Nucl. Phys. **A316**, 253 (1979).
[198] A. Dar and Z. Kirzon, Phys. Lett. **37B**, 166 (1971).
[199] Z. Kirzon and A. Dar, Nucl. Phys. **A237**, 319 (1975).
[200] V. S. Barashenkov, É. S. Gavrilov, and S. M. Eliseev, Preprint R2-6423 [in Russian], JINR, Dubna (1972); V. S. Barashenkov and Zh. Zh. Musul'manbekov, Preprint R2-11453 [in Russian], JINR, Dubna (1978).
[201] C. K. Varna, Phys. Rev. C **17**, 267 (1978).
[202] A. N. Antonov, I. S. Bonev, V. A. Nikolaev, and I. Zh. Petkov, Communication R4-12633 [in Russian], JINR, Dubna (1979).
[203] A. I. Akhiezer and I. Ya. Pomeranchuk, Zh. Eksp. Teor. Fiz. **16**, 396 (1946).
[204] S. A. Karamyan, Yu. Ts. Oganesyan, Yu. É. Penionzhkevich, and B. I. Pustyl'nik, Preprint R7-5884 [in Russian], JINR, Dubna (1971).
[205] A. N. Antonov, L. P. Kaptari, V. A. Nikolaev, and A. Yu. Umnikov, Rapid Communication No. 2 [41]-90, JINR, Dubna (1990), p. 14.

Translated by Julian B. Barbour